Climate change, fire return intervals and the growing risk of permanent forest loss in boreal Eurasia

Arden L. Burrell[1,2*] *aburrell@woodwellclimate.org

Qiaoqi Sun[3,4]

Robert Baxter[3]

Elena A. Kukavskaya[5]

Sergey Zhila[5]

Tatiana Shestakova[1]

Brendan M. Rogers[1]

Jörg Kaduk[2]

Kirsten Barrett[2]

1. Woodwell Climate Research Center, Falmouth, MA, United States of America
2. Centre for Landscape and Climate Research, School of Geography, Geology and Environment, University of Leicester, University Road, LE1 7RH, UK
3. Department of Biosciences, University of Durham, Upper Mountjoy, South Road, Durham, DH1 3LE, United Kingdom.
4. College of Wildlife and Protected Area, Northeast Forestry University, 26 Hexing Road, Harbin 150040, China
5. V.N. Sukachev Institute of Forest of the Siberian Branch of the Russian Academy of Sciences - separate subdivision of the FRC KSC SB RAS, 660036 Russian Federation, Krasnoyarsk, Akademgorodok 50/28.

Abstract

Climate change has driven an increase in the frequency and severity of fires in Eurasian boreal forests. A growing number of field studies have linked the change in fire regime to post-fire recruitment failure and permanent forest loss. In this study we used four burned area and two forest loss datasets to calculate the landscape-scale fire return interval (FRI) and associated risk of permanent forest loss. We then used machine learning to predict how the FRI will change under a high emissions scenario (SSP3-7.0) by the end of the century. We found that there are currently 133 000 km^2 forest at high, or extreme, risk of fire-induced forest loss, with a further 3 M km^2 at risk by the end of the century. This has the potential to degrade or destroy some of the largest remaining intact forests in the world, negatively impact the health and economic wellbeing of people living in the region, as well as accelerate global climate change.

1. Introduction

Boreal forests contain ~30 % of all of the world's forested area (Gauthier et al., 2015), ~65% of the world's forest carbon stocks (Bradshaw and Warkentin, 2015), contribute ~20 % of the world's terrestrial carbon sink (Bradshaw and Warkentin, 2015; Pan et al., 2011) and include some of the largest areas of intact forest in the world (Potapov et al., 2017). Warming rates in the boreal region are among the fastest in the world (D'Orangeville et al., 2018), which has increased vegetation productivity (Chen et al., 2016; Goetz et al., 2005; Kauppi et al., 2014; Keenan and Riley, 2018; Liu et al., 2015) and driven the expansion of boreal species to higher altitudes and north into the tundra (Brodie et al., 2019; Forbes et al., 2010; Myers-Smith et al., 2011; Suarez et al., 1999). There is growing concern, however, that climate change is causing a reduction along the southern boundary with the steppe biome, especially in more water-limited forests (Guay et al., 2014; Huang et al., 2010; Koven, 2013; Payette and Delwaide, 2003).

Wildfire is one of the largest causes of stand mortality in boreal forests, a natural dynamic which has been in place for thousands of years (Johnstone et al., 2010; Kharuk et al., 2021; Ponomarev et al., 2016). As a result, many regions have been in a dynamic equilibrium, whereby the amount of ecosystem carbon lost to wildfire, determined by factors such as the Fire Return Interval (FRI) and the portion of stand-replacing fires, is balanced by the rate of recovery (Brazhnik et al., 2017; Brown and Johnstone, 2012). In these regions, periodic fires play an essential role in maintaining ecosystem health and biodiversity (Kharuk et al., 2021). However, at the southern limits of the Eurasian boreal zone, there is growing evidence of recruitment failure (RF) driven forest loss (Barrett et al., 2020; Kukavskaya et al., 2016). RF is where boreal tree species fail to re-establish after a stand-replacing disturbance and instead undergo a change to a steppe/grassland (Barrett et al., 2020).

Although the conditions that cause RF are complex and multifaceted, certain drivers such as the FRI and the percentage of stand-replacing fires have distinct thresholds beyond which RF is highly likely (Hansen et al., 2018; Kukavskaya et al., 2016; Stevens-Rumann et al., 2018). For example, in the first 20-30 years after a stand replacing fire, the regenerating tree species have almost no fire tolerance and contribute very little to the seed pool, which is essential for robust post-fire recruitment (Cai et al., 2018; Hansen et al., 2018; Kukavskaya et al., 2016). For this reason, the interval between a stand-replacing fire and the next fire event is one of the strongest predictors of RF within the boreal zone (Kukavskaya et al., 2016; Whitman et al., 2019).

Although the global extent of RF remains entirely unquantified (Burrell et al., 2021), it has been observed in field studies from both the Eurasian (Barrett et al., 2020; Kukavskaya et al., 2016;

Shvetsov et al., 2019) and North American boreal forest (Boucher et al., 2019; Brown and Johnstone, 2012; Hansen et al., 2018; Stevens-Rumann et al., 2018). In a study of 1538 field sites across boreal North America, post-fire RF was observed at ~10% of sites (Baltzer et al., 2021) though it should be noted that the link between RF and forest loss is less certain in the mixed broadleaf and coniferous forests of North America (Gill et al., 2017; Johnstone and Chapin, 2006; Whitman et al., 2019), than it is in the coniferous forests of Eurasia (Barrett et al., 2020; Burrell et al., 2021; Kukavskaya et al., 2016). If RF and its associated forest loss is widespread, this poses a serious risk to the wealth of ecosystem services provided by boreal forests (Gauthier et al., 2015; Hansen et al., 2013). It would also negatively impact the boreal carbon sink, potentially leading to a net source, which would further amplify climate change (Chen and Loboda, 2018; Hayes et al., 2011; Lin et al., 2020).

Eurasia contains some of the hottest and driest parts of the boreal biome and is warming faster than the global average (Burrell et al., 2021). Given the influence of fuel availability, fire season length, and fire weather, there are direct links between burned area and climatology, as well as climate changes in Siberia (de Groot et al., 2013; Kharuk et al., 2021; Tepley et al., 2018). The Eurasian boreal biome has already experienced an extension of the fire season, increases in fire frequency, extent and severity – including increased proportions of fires that are stand replacing (Brazhnik et al., 2017; Feurdean et al., 2020; Kharuk et al., 2021; Malevsky-Malevich et al., 2008; Ponomarev et al., 2016; Tomshin and Solovyev, 2021). As the climate continues to warm, this trend is likely to continue (Malevsky-Malevich et al., 2008; Shvetsov et al., 2016), with the Sixth Assessment Report of the United Nations Intergovernmental Panel on Climate Change (IPCC) predicting increase in fire frequency and severity across all of Eurasia (IPCC, 2021). Given the strong link to climate change, the growing evidence of site-level RF, the threat it poses to boreal carbon sink and the limited knowledge over large areas, quantifying the extent of RF in the boreal forest as a key knowledge gap in the boreal zone (Baltzer et al., 2021; Burrell et al., 2021).

The reason the extent of RF remains unknown is because of a lack of the data and methods needed to systematically quantify it at large scales (Burrell et al., 2021). The ideal method to measure post-fire RF would involve a large number of field sites with >30 years of tree cover data, which does not currently exist for many parts of the often very remote boreal zone, with the data availability in Siberia, for example, being especially low (Burrell et al., 2021). Another option for quantifying RF would be to directly detect it using remotely sensed imagery, or by proxy using remotely sensed data products to construct site-level fire histories. Such histories can indicate where the gap between a stand-replacing fire and the subsequent fire event was less than the 30-year threshold observed in field studies of recruitment (Hansen et al., 2018; Kukavskaya et al., 2016). To the best of our knowledge, there have been no studies that have done this at a large spatial scale. This is likely because performing the analysis over a large area would require high spatial resolution data with a temporal record that is longer than is currently available (Burrell et al., 2021; Chu and Guo, 2014). Existing studies using remote sensing to look at post-fire forest recovery generally only assess recovery in the first 5 years after fire (Frazier et al., 2018). Given that site-level fire/disturbance histories extending beyond the satellite period are unavailable in most areas, landscape-scale FRI, calculated using a space for time substitution, has been used to investigate ecosystem changes driven by wildfire (Coops et al., 2018; Kharuk et al., 2021; Soja et al., 2006; Tomshin and Solovyev, 2021).

The Russian Far East and Siberian portions of the boreal zone have been the focus of notably fewer research studies than either the North American or Scandinavian boreal forest (Rogers et al., 2020). This is particularly problematic because the climatology and current rates of warming in Siberia suggest that the changes occurring in this region may be truly indicative of the future of the boreal zone as the climate warms (Burrell et al., 2021). These are also the regions with multiple studies showing RF induced forest loss (Barrett et al., 2020; Kukavskaya et al., 2016; Shvetsov et al., 2019).

The aim of the present study was to use freely available remotely sensed datasets to investigate landscape-scale FRI, stand replacing FRI (FRI_{SR}) and the all-cause Disturbance Return Interval (DRI) which together can be used as a proxy for RF risk and, by association, the areas most at risk of permanent biome shift in the Eurasian boreal forest. Machine learning methods were then used to examine the link between FRI and climate over the observed period and, in combination with future climate projections, to quantify how this risk will change over the next century.

2. Materials and Methods

2.1 Study Area

The analysis was performed over the entire Eurasian boreal forest, a region containing ~15 M km^2 of forest dominated by a small number of tree species from four main genera, larch (*Larix*), pine (*Pinus)*, birch (*Betula*), and spruce (*Picea*) (Bartalev et al., 2004; de Groot et al., 2013; Rogers et al., 2015) (Figure 1).

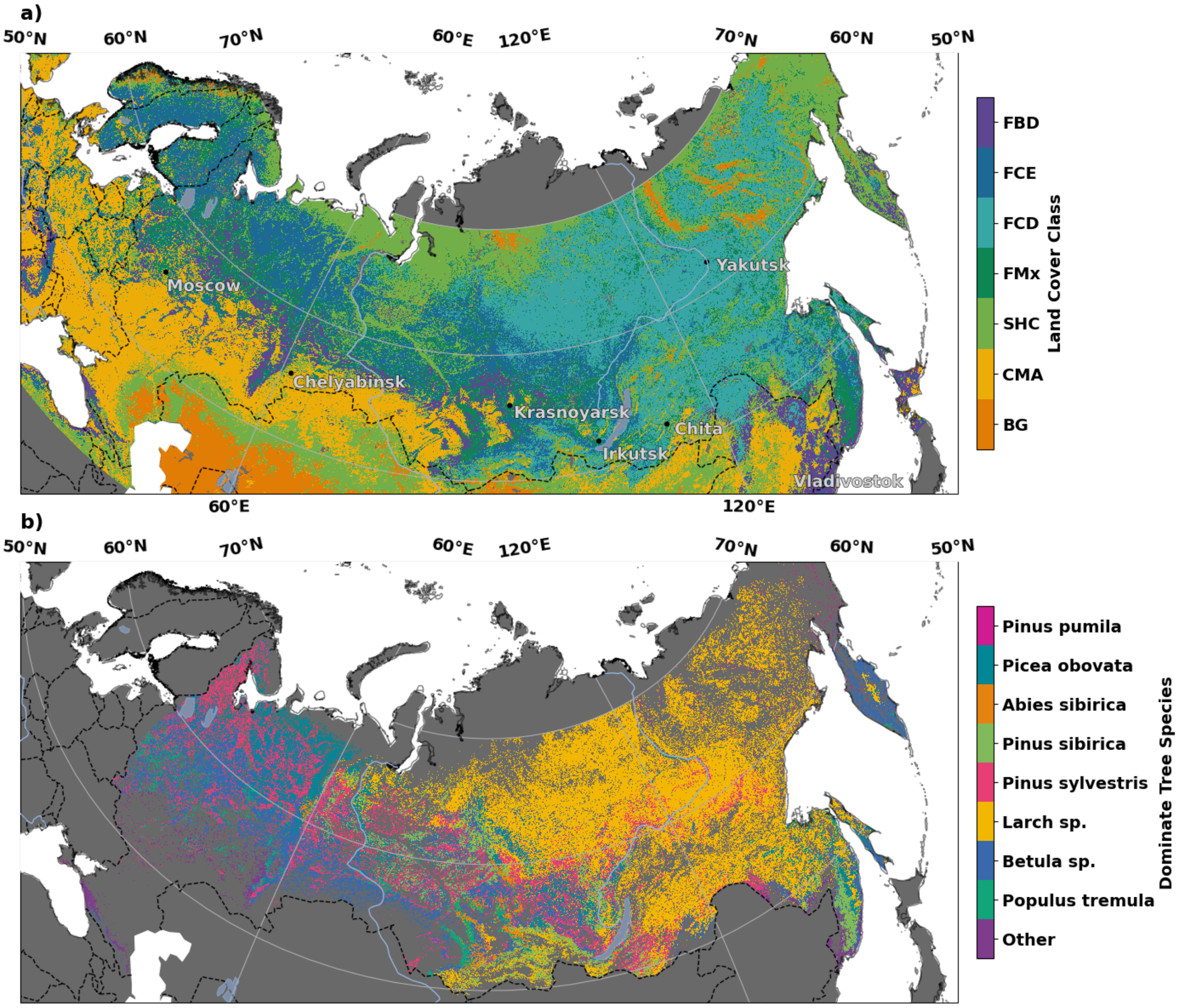

Figure 1. Land cover types. *a) The dominant land cover class in the year 2000 (FBD: Broadleaf Deciduous Forest, FCE: Coniferous Evergreen Forest, FCD: Coniferous Deciduous Forest, FMx: Mixed Forest, SHC: Shrubs and/or Herbaceous Cover, CMA: Cultivated and/or Mixed Agriculture, BG: Bare Ground). b) The dominant tree species. Data: a) GLC2000 (Bartholomé and Belward, 2005) and b) adapted from (Bartalev et al., 2004).*

As this study focuses on the shift of the boreal-steppe boundary and existing static boreal forest maps may be misleading due to shifts in this boundary, we derived the boreal biome boundary using forest cover data rather than using an existing biome map. We used version 1.7 of the Hansen Global Forest Change (HansenGFC) 2000 tree cover data (Hansen et al., 2013) to identify the boreal-steppe boundary and mask out non-forested areas in all datasets. For this study we included any area located between 40° to 70° of latitude and -10.0° to 180° of longitude that had a fractional tree cover greater than 10 %. To exclude the temperate forests that occur in these regions, we then used boreal ecoregions from Dinerstein et al. (2017) with a 1° buffer to account for any uncertainties in the boundaries.

2.2 Burned Area Datasets

In order to partially control for the uncertainties and biases in any one data source, we used four global Burned Area (BA) products to estimate FRIs in Eurasian boreal forests (Table 1). The first, the Moderate Resolution Imaging Spectroradiometer (MODIS) Collection 6 Burned Area product (MCD64A1), is the most widely used and validated global BA dataset (Giglio et al., 2018). The second is the fourth version of the Global Fire Emissions Database 4.1 (GFED4) BA (including small fires) (van der Werf et al., 2017), which is mostly based on MODIS MCD64A1 data (Randerson et al., 2017). The 'small fires' version of GFED4 incorporates a correction to address the known bias in BA products of underrepresenting the extent and frequency of smaller and/or low intensity fires (Randerson et al., 2012). It was included in this study because it is comparable to the lower resolution datasets that have previously been used to examine FRI in Eurasia. The third is the European Space Agency's Climate Change Initiative FireCCI version 5.1 (FireCCI51), which uses MODIS spectral and active fire data, and was designed to improve the accuracy over MCD64A1 (Lizundia-Loiola et al., 2020). The fourth is the Copernicus Global Land Service BA product (CGLS-BA) which is derived from PROBA-V data (Smets et al., 2017). In comparison to other products, the performance of CGLS-BA is expected to be worse than other products in the boreal zone because it cannot detect any spring or autumn fires north of 51^{o}, but we included it in this study because it is the only high-resolution global BA product that is currently being updated and is entirely independent of MODIS data.

In addition to the BA products, we also used version 1.7 of the 25 m Hansen Global Forest Change (HansenGFC) dataset to estimate forest loss rates due to fire (Hansen et al., 2013). HansenGFC v1.7 uses Landsat 8 for improved detection of boreal forest loss, including from fire. However, this correction is not applied to the years 2001 to 2010. To examine the rate of forest loss due to fires, we followed the procedure used by Krylov et al. (2014) and used MODIS active fire data (MCD14ML) to mask out areas where forest loss does not occur within 4 km of a fire (HansenGFC-MAF). HansenGFC-MAF is the subset of the forest loss in HansenGFC that can be attributed to fires, and therefore represents only stand replacing fires.

Table 1 Summary of gridded datasets used

Product	Dataset type	Resolution	Temporal range	Citation
MCD64A1	Burned Area	~500 m	2001 to present	Giglio et al. (2018)
GFED4	Burned Area	0.25-degree (~27 km at the equator)	1996 to 2017	van der Werf et al. (2017)

FireCCI51	Burned Area	~250 m	2001 to present	Lizundia-Loiola et al. (2020)
CGLS-BA	Burned Area	~300 m	2014 to present	Smets et al. (2017)
HansenGFC	Forest loss	25 m	2001 to present	Hansen et al. (2013)
TerraClimate	Precipitation and Temperature	~4 km	1984 to present	Abatzoglou et al. (2018)

2.3 Calculating landscape-scale FRI

Estimating site-level FRI requires long-term observations with multiple fire events, typically from sediment cores, tree rings from surviving trees or long-term site monitoring; information that is not publicly available for most of the Eurasian boreal forest zone. FRI can also be calculated at regional and continental scales using space-for-time substitution, assuming homogeneity in FRI at a particular spatial scale (Archibald et al., 2013). Because all the moderate and high spatial resolution BA products currently available have insufficient temporal record for the majority of site-level FRI's in Eurasian boreal forests, we adopted this latter approach. For the four BA datasets (GFED4, FIreCCI51, MCD64A1 and CGLS-BA), we calculated the fire frequency for each forested pixel and then applied a 1 degree moving window (excluding non-forest areas) to calculate the landscape-scale mean annual burned fraction (AnBF). *AnBF* for a given pixel is calculated using:

1. $$AnBF = \frac{\left(\sum_{yr=ys}^{yf}\left(\frac{BA_{yr}}{FC}\right)\right)}{yf-ys+1}$$

where *ys* is the first year of the dataset, *yf* is the last year of the dataset, BA_{yr} is the total area burned in a given year (*yr*) in a 1° box around the pixel, and *FC* is the total area covered by forest in the 1° box around the pixel. The 1° moving window was chosen after preliminary testing which found that a smaller window (0.5°) was highly sensitive to noise, while larger windows (2° and 5°) resulted in very similar results as 1° but at greatly increased computing cost. This moving window also minimises the impact of differences in the resolution of the input datasets as it is a courser resolution than all of the datasets used.

The landscape FRI was then calculated by taking the reciprocal of the AnBF. This procedure was also applied to both the HansenGFC and HansenGFC-MAF to calculate the Disturbance Return Interval (DRI) and the FRI_{SR} respectively, after upscaling these products from their native 25 m resolution to 250 m (the same grid as FireCCI). The DRI is the return interval for all stand replacing disturbances and includes stand replacing fires, logging and wind disturbance while the FRI_{SR} is return interval for the subset of stand replacing disturbances that are linked to fire. For all datasets we used the full temporal record available at time of analysis (2001 to 2018 for FIreCCI51, MCD64A1, HansenGFC and HansenGFC-MAF; 1997 to 2018 for GFED4; and 2014 to 2018 for CGLS-BA) which may account for some of the differences between the estimated FRI's.

While stand-replacing fires temporarily reduce the risk of subsequent fire events by reducing fuel loads (Bernier et al., 2016; Beverly, 2017; Erni et al., 2018; Walker et al., 2020), this effect appears to be relatively short-lived in Siberia because of the rapid recovery of flammable understory grasses (Kukavskaya et al., 2014), with studies showing that wildfire can occur in a forest of any stand age, composition or canopy density (Brazhnik et al., 2017; Hansen et al., 2013; Kukavskaya et al., 2016). This dynamic has also been observed in western Canada (Stralberg et al., 2018). Given this, and assuming that a proportion of fires are stand-replacing (Section 2.4.2), the landscape FRI indicates how long a forest has between a stand replacing fire and the next fire event.

Using a space-for-time substitution to calculate FRI becomes much less accurate in areas with long FRI's (small AnBF's) (Archibald et al., 2013; Falk et al., 2007). In these areas the addition of a single fire event can make a large difference in the calculated FRI. For this reason, we only report FRI up to 10 000 years. Beyond FRI's of 10 000 years, single pixel decreases in AnBF result in exponential increases in the estimated FRI. As such, areas with FRI >10 000 years were also excluded from the modelling of FRI.

2.4 Selection of critical thresholds

Our thresholds for permanent forest loss risk were selected by combining the FRI, which is the frequency a location experiences a fire of any intensity, with both the FRI_{SR} and DRI, which provide information on disturbance dynamics and by association stand age. In the present study we used thresholds of landscape FRI as a proxy for the risk of permanent forest loss with <15 years indicating extreme risk and 15 to 30 years indicating high risk, while for the DRI and $FRI_{SR.}$ the extreme risk threshold was <60 years and 60 to 120 years for high risk. When the FRI risk group is used in combination with the FRI_{SR}/DRI risk group, it is possible to estimate how likely an area is to experience a burn during the vulnerable establishment phase of recovery and therefore assign a risk category. A full justification of the thresholds and combined risk categories is described below.

These thresholds for both the FRI and FRI_{SR}/DRI were selected based upon information from Scots Pine (*Pinus sylvestris*) stands, which have been studied in the context of recruitment failure and represent the dominant tree species in parts of the Eurasian boreal forest with the highest levels of drought and shortest FRI's (Shvetsov et al., 2019). This suggests a fire regime that excludes Scots pine is highly likely to exclude all other boreal tree species such as larch (*Larix* spp.) and dark taiga (*Picea* and *Abies* spp.) (Schulze et al., 2012). Applying the procedure detailed above to larch gives FRI thresholds that are equal to, or greater than, those for Scots pine

2.4.1 FRI thresholds

We used two primary sources of ecological information on *Pinus sylvestris* to establish our risk thresholds. The first is the relationship between stand age and seed production, and the second is the relationship between stand age and fire-induced tree mortality. Whilst high severity crown fires result in high to total mortality of trees regardless of age and DBH, the probability of mortality for a tree in low-severity surface fires is directly associated with its width, or diameter at breast height (DBH): for example the probability of fire-induced mortality is 80 to 100 % for trees with DBH <10 cm, 14 % for DBH from 10 to 20 cm and 1.4 % for trees with a DBH of 40 to 50 cm (Kukavskaya et al., 2014; Linder et al., 1998). As for the relationships between stand age and seed production, it generally takes between 5 and 15 years after a stand-replacing fire for trees to produce seeds that begin to replenish the seedbank (Sullivan, 1993; Wright et al., 1967). This initial seed production is generally very limited, with the first large seeding events not occurring until the trees reach 25 to 30 years of age (Broome et al., 2016).

Trees less than 15 years old almost always have a DBH < 10 cm, meaning any fires that occur within that period will kill almost all the saplings, and with little to no seedbank, a transition to a non-forested ecosystem is almost guaranteed unless the stand is immediately adjacent to a seed source (Chmura et al., 2012; Kukavskaya et al., 2014; Linder et al., 1998). Multiple field studies have observed RF if an area burns again <15 years after a stand-replacing fire (Kukavskaya et al., 2016, 2016; Shvetsov et al., 2016). While the stand age vs DBH relationship varies considerably between regions, in general stands 30 years old will have DBHs between 10 and 20 cm, which means they have ~80 % chance of surviving a low-severity surface fire but remain vulnerable to moderate and high severity fires (Linder et al., 1998; Sidoroff et al., 2007; Sullivan, 1993). It should be noted that the estimates of DBH vs age are often based on plantations and as such represent an upper limit on growth rate. Looking at natural forests, there are many sites with average DBH below 20 cm more than 100 years after the stand replacing fire (Edwards and Mason, 2006; Sandström et al., 2020; Stavrova et al., 2020). We chose 15 to 30 years as our second critical threshold due to both the high mortality rate and lower seed availability before the first mass seeding event.

It should be noted that while we used Scots pine to represent a reasonable lower bound of the FRI survivability of boreal tree species, our thresholds are consistent with those found in studies of post-fire RF in similar ecosystems with different dominant species across the globe (Baltzer et al., 2021;

Hansen et al., 2018; Stevens-Rumann et al., 2018). For example, in a study of RF in the alpine region of the continental USA, the serotinous lodgepole pine (*Pinus contorta*), a species whose first large seeding event occurs at 15 years of age (Broome et al., 2016), only failed to establish when FRIs were <20 years and stands were far (>1 km) from a seed source (Hansen et al., 2018).

2.4.2 DRI and FRI_{SR} thresholds

If all the fires observed in an area are low severity surface fires with little to no fire-induced stand mortality, then FRI cannot be used as a proxy for ecosystem risk. Even though most fires in the Siberian boreal forests are surface fires (Rogers et al., 2015) this non-stand-replacing fire dynamic is not common in most coniferous forests. It has been, however, observed in the broadleaf forest along the boreal-temperate boundary (Krylov et al., 2014; Schulze et al., 2012). A similar dynamic has also been observed in some mature Scots pine forest stands in southern Siberia with FRI's of 20 to 40 years, but less than 10% of fires being high mortality crown fires (Kharuk et al., 2021). To account for the influence of low-severity surface fires versus stand-replacing fires, we compared the DRI and FRI_{SR} from HansenGFC and HansenGFC-MAF data, respectively. The FRI_{SR} is always equal or longer than DRI because HansenGFC-MAF is a subset of the HansenGFC data. DRI is included in the risk framework because non-fire disturbances like logging can act in place of a stand replacing fire to start the recovery phase and because they have been shown to significantly increase the likelihood of RF (Kukavskaya et al., 2014; Perrault-Hébert et al., 2017; Shvetsov et al., 2021).

In the Eurasian boreal zone, conifer species generally experience a FRI of between 30 to 50 years and FRI_{SR} around 200 years (120 to 300 years), though FRI_{SR}'s as low as 60 years have been observed in some of the southern boreal regions (Kharuk et al., 2021, 2016; Schulze et al., 2012). We chose <60 years as our extreme threshold as it is the lowest value observed in stable forests, with 60 – 120 years being high risk as 120 years is the bottom of the normal range and is also close to when Scots pine transition from early to mid-stage successional dynamics (Stavrova et al., 2020). Given that regenerating forests are highly vulnerable to reburning for the first 30 years, a DRI/FRI_{SR} of 60 years means a that a forest spends ~50% of its time being vulnerable to fire induced RF, while a DRI/FRI_{SR} of 120 years means a forest spends ~25% of the time being vulnerable.

2.4.3 Combined risk framework

The forest risk framework works by combining the DRI/FRI_{SR} thresholds of <60 years for extreme risk and <120 years for high risk, with the FRI thresholds of <15 years for extreme risk and < 30 years for high risk to determine the risk of forest loss. An area is considered low risk if it is not in the high or extreme risk groups for both FRI and DRI/FRI_{SR}, moderate risk is either FRI or DRI/FRI_{SR} is high/extreme risk but not the other, high risk is where both FRI and DRI/FRI_{SR} are high risk but neither is extreme risk, and extreme risk if either FRI or DRI/FRI_{SR} is extreme risk and the other is high or extreme risk. The combined risk framework also makes a distinction between the different risks caused by the dominant driver of stand replacement. In cases where the FRI_{SR} and the DRI risk group are the same, then fire must be the dominate cause of disturbance and the risk driver. When the DRI group is a higher than the FRI_{SR} risk group, it indications that process like logging or insect predation are increasing the risk of RF induced forest lost. The full risk criteria are described in Table 2.

Table 2 *Thresholds used to determine forest loss risk and resulting risk classes. All numbers represent years. The dominant driver is listed in parentheses with dist indicating disturbance.*

	FRI_{SR}<60	**FRI_{SR} 60-120**		**FRI_{SR}>120**		
	DRI<60 (extreme)	**DRI<60 (extreme)**	**DRI 60-120 (high)**	**DRI<60 (extreme)**	**DRI 60-120 (high)**	**DRI>120 (Low)**
FRI<15 (extreme)	Extreme Risk (fire)	Extreme Risk (dist)	Extreme Risk (fire)	Extreme Risk (dist)	Extreme Risk (fire)	Moderate Risk (fire)
FRI 15-30 (high)	Extreme Risk (fire)	Extreme Risk (dist)	High Risk (fire)	Extreme Risk (dist)	High Risk (dist)	Moderate Risk (fire)
FRI>30 (low)	Moderate Risk (fire)	Moderate Risk (dist)	Moderate Risk (fire)	Moderate Risk (dist)	Moderate Risk (dist)	Low Risk

This analysis and the risk framework are both predicated on the assumption that errors in the BA products do not have high commission error bias. Accuracy assessments of BA products have found large errors with a strong omissions bias and a tendency to greatly underrepresent low severity surface fires in the boreal zone (Brennan et al., 2019; Giglio et al., 2018; Humber et al., 2019; Lizundia-Loiola et al., 2020). This would indicate that the actual landscape-scale FRI might be significantly shorter than that found in this study. We also performed a small, independent, accuracy assessment at 50 field sites in the Zabaikal region of southern Siberia the method and results of which are included in Supplementary Text 1 and Supplementary Figure 1 and 2.

2.5 Modelling the relationship between FRI and the climatology

To model the relationship between FRI and climatology, we applied two machine learning approaches. The first was a simple multivariate regression implemented using the scikit-learn python library (Pedregosa et al., 2011), and the second was as an Extreme Gradient Boosted regression implemented using XGBoost (Chen and Guestrin, 2016). To look at the relationship between FRI and climatology we used the TerraClimate gridded monthly temperature and precipitation data (Abatzoglou et al., 2018) as well as the TerraClimate predicted future climate (Qin et al., 2020). TerraClimate is a ~4 km global dataset of monthly climate variables created by combining multiple existing gridded and remotely-sensed climate data products (Abatzoglou et al., 2018).

To calculate our observed climatology, we used TerraClimate precipitation and temperature data (Abatzoglou et al., 2018). For each year we calculated the accumulated precipitation and the monthly mean temperature for the meteorological seasons (December-February (DJF), March-May (MAM), June-August (JJA), September-November (SON)). The seasonal climatology was then calculated by taking the mean over the 31 years from 1985 to 2015. This time period was chosen because it is long enough to account for natural climate variability (Burrell et al., 2020), has a significant overlap with all the BA datasets, and is directly comparable with the TerraClimate predicted future climate (Qin et al., 2020).

To calculate the relationship between FRI and seasonal climatology, the climate dataset was resampled to the same grid as the FRI dataset being tested using a second order conservative remapping using the Climate Data Operators software package (Schulzweida, 2020). Then we applied the same 1^o x 1^o moving window to climate data as we used to calculate the FRI. To avoid training and testing the machine learning models on spatially autocorrelated data, one pixel was selected from each 1^o x 1^o grid cell (~110 km^2). We then excluded areas with less than 10% forest cover as well as areas with landscape FRI >10 000 (section 2.3).

We used mean Annual Burned fraction as a dependent variable because initial trials showed better model performance predicting AnBF and then converting to FRI compared to models that predict FRI directly. This is probably because machine learning methods perform better on variables that are scaled between 0 and 1 (Wan, 2019; Zheng and Casari, 2018). For independent variables, we used the seasonal precipitation and temperature climatology as well as the mean tree cover fraction in the year 2000 derived from Hansen GFC dataset (Hansen et al., 2013). These independent variables were pre-processed using a Quantile Transform. We then used Python's Scikit-learn package (Pedregosa et al., 2011) to perform an 80:20 train-test split with the 20% remaining withheld to assess out-of-sample accuracy.

The accuracy of the models was assessed by calculating the R^2 on the fully withheld testing values. We then applied these trained models to every pixel at the native resolution of the BA product. This process was applied to all four BA datasets. In the case of the XGBoost models, the importance of different variables was also determined using Feature Importance and Permutation Importance tests.

2.6 Determining the climate change-driven trends and estimating future FRI

To estimate future FRI, we used the recently developed TerraClimate predicted future climate (Qin et al., 2020), which uses a 23-member climate model ensemble to generate a realistic climate dataset for the period 2085 to 2115 under Shared Socioeconomic Pathways (SSP)3 – 7.0 emissions. Because of the known issues with CMIP model predictions of precipitation like the widely documented *"drizzle problem*" (Abdelmoaty et al., 2021; Akinsanola et al., 2020; Chen et al., 2021; Coppola et al., 2021; Srivastava et al., 2020), we also created three predicted climatologies for the periods 2015 to 2045, 2045 to 2075, and 2085 to 2115 by adding the climate change-driven trend to the observed 1985-2015 climatology.

Calculating the climate change-driven trend in regions with high natural climate variability, such as the boreal steppe transition zone in Siberia, requires removing the inherent interannual and inter-decadal climate variability (Burrell et al., 2020, 2019). To do so, we used the process outlined in Burrell et al. (2020), whereby a 20-year leading edge moving average smoothing (sometimes called a Simple Moving Average) was applied to each pixel to remove interannual climate variability. Using a moving window smoothing to separate variability and trend components is standard practice in time series analysis and is widely used when working with climate time-series data (Abram et al., 2020; Ahmed et al., 2018; Bläsche et al., 2014). A Theil-sen Slope estimator (Theil, 1950) was then applied to calculate the climate change-driven shift in seasonal temperature and precipitation over the period 1985 to 2015 with a Spearman's rank correlation co-efficient test used to measure statistical significance for each pixel (Yue et al., 2002). The Benjamini–Hochberg procedure was then applied to the p-values from the Spearman's rank correlation co-efficient test to control for False Discovery Rate (FDR) ($\alpha_{FDR} = 0.10$), which accounts for multiple testing and spatial autocorrelation issues (See (Wilks, 2016) for details). FDR testing ($\alpha_{FDR} = 0.10$) is more rigorous and more robust than the more commonly used p-value test ($\alpha_{p\text{-value}} = 0.05$) alone (Wilks, 2016). We then used the observed climate change driven trend and the significant trends to estimate future climatology. Non-significant trends were not included. All the climatology datasets were prepared in the same manner as detailed in section 2.5, and the models trained over the observed period (1985 to 2015) were applied to create estimates of future FRI. We then calculated the future fire-induced forest loss risk using the predictions of FRI and the fire risk criteria detailed in Table 2. The calculation of future forest loss risk assumes that the proportion of fires that were stand replacing remained constant though time for a given location.

3. Results

3.1 Current Fire Return Interval (FRI)

Looking at the large-scale patterns in FRI between the BA datasets (Figure 2), FRI's calculated from the three MODIS-derived BA datasets (GFED4, MCD64A1, FireCCI51) show similar spatial patterns with the shortest FRI's observed along the southern boundary of the Eurasian boreal forest, as well as the forests around Yakutsk. There is less agreement between CGLS-BA and the MODIS-derived BA products, with large differences along the northern tundra/boreal border, as well as in Far East along the China-Russia border north of Vladivostok (Figure 2). These patterns are also apparent in the median (1st, 99th percentile) FRI, with 446 yrs (20 yrs, >10,000 yrs) for GFED4, 549 (17 yrs, >10,000 yrs) for MCD64A1, 501 (9yrs, >10,000yrs) for FireCCI51 and 319 yrs (21 yrs, >10,000 yrs) for CGLS-BA. Looking at the areas with the shortest FRI's, our results indicate that between 0.2% and 2.4% (GFED4: 32,011 km^2, MCD64A1: 65,356 km^2, FireCCI:225,932 km^2, CGLS-BA: 21,114 km^2) of the Eurasian boreal zone that was forested in 2000 has experienced an FRI <15 years. In addition, there is a further 2.2% to 3.3% of forests with FRI's between 15 to 30 years (GFED4: 215,612 km^2, MCD64A1: 269,934 km^2, FireCCI: 255,931 km^2, CGLS-BA: 347,181 km^2).

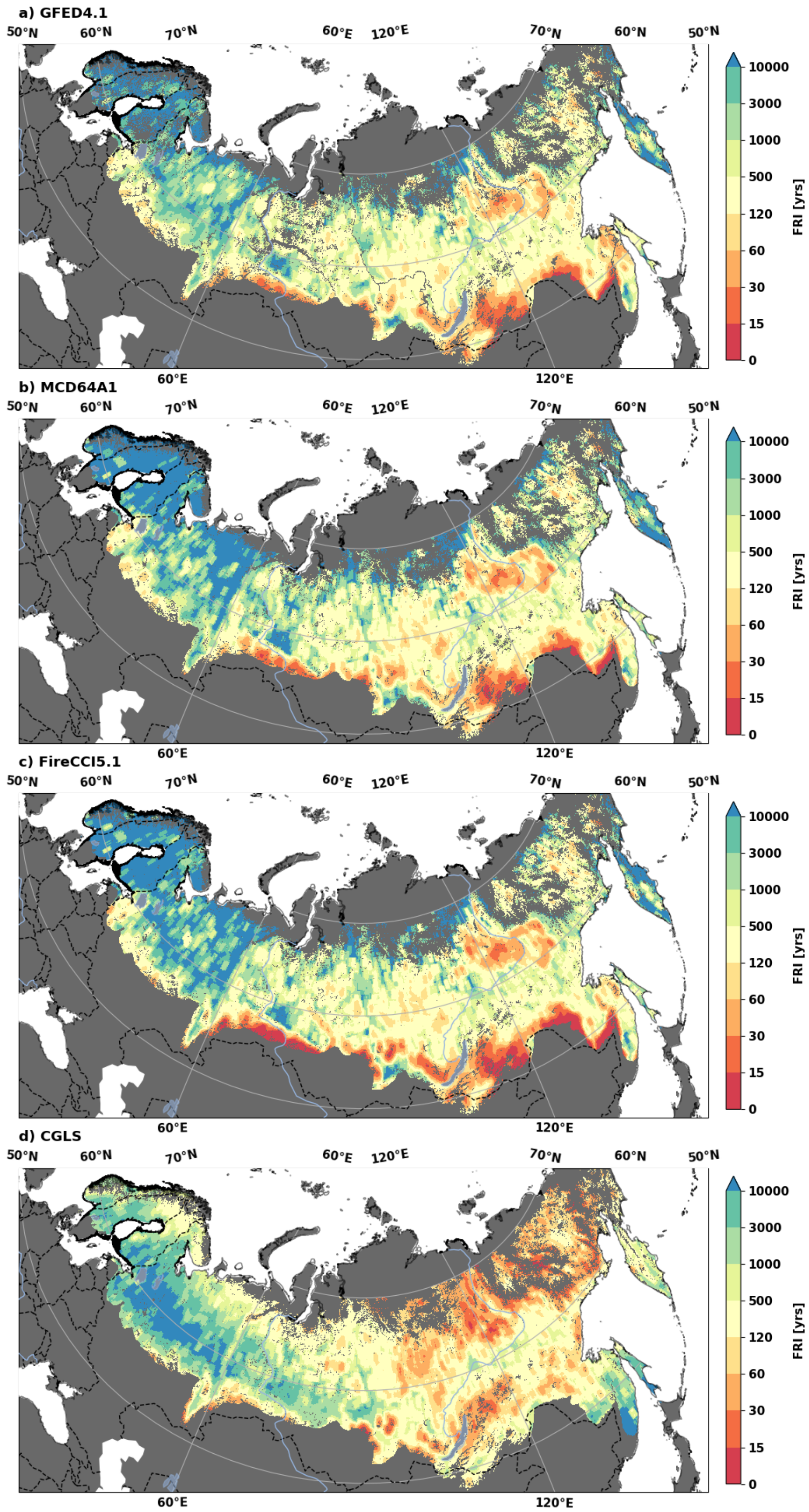

Figure 2 Maps of the landscape-scale Fire Return Interval (FRI) *in years calculated using a 1° x 1° moving window applied to four Burned Area (BA) datasets: a) GFED4; b) MCD64A1; c) FireCCI51, and d) CGLS-BA. Non-Boreal Forest regions are masked in grey.*

3.2 Current FRI_{SR} and DRI

Looking at the all-cause Disturbance Return Interval (DRI) and stand-replacing Fire Return Interval (FRI_{SR}), we find that fire accounts for about 63.7% of the forest loss in the Hansen global forest cover dataset. Over the Eurasian boreal forest, the median (1^{st}, 99^{th} percentile) FRI_{SR} was 1302 yrs (59 yrs, >10,000 yrs) while the DRI was 367 yrs (52 yrs, >10,000 yrs). Comparing SR and DRI spatially, fire is the dominant driver ($FRI_{SR} \approx DRI$) of disturbance in eastern Eurasia, while in the western half of the region DRI is much shorter than FRI_{SR} which indicates that logging, wind or other drivers are the dominant causes of disturbance. The DRI with fire removed is included in Supplementary figure 3.

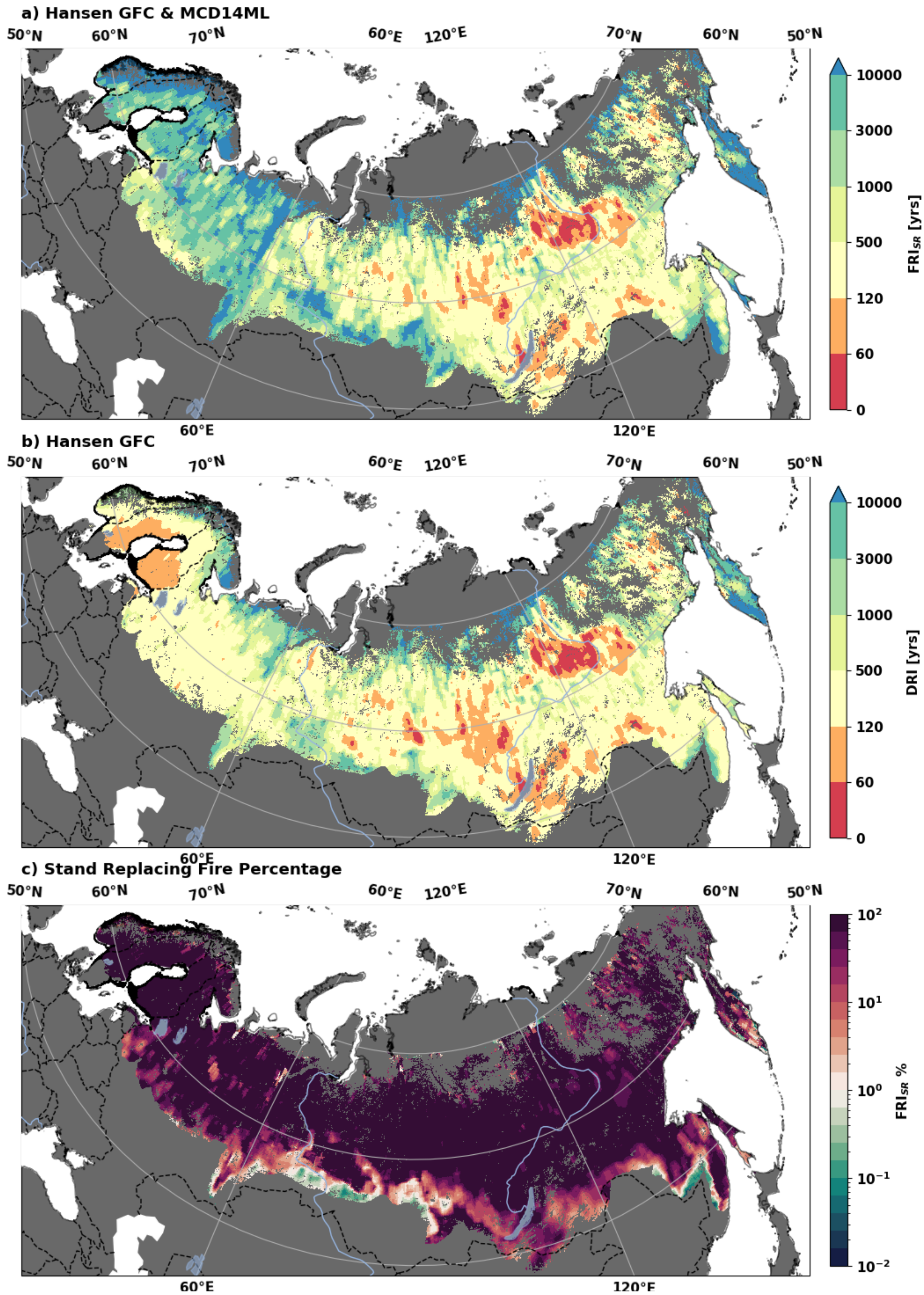

Figure 3 Rates of Forest loss *a) The stand-replacing Fire Return Interval (FRI$_{SR}$) calculated using HansenGFC-MAF (Krylov et al., 2014); b) the Disturbance Return Interval (DRI) calculated using HansenGFC (Hansen et al., 2013); c) The percentage of fires that are stand-replacing calculated by dividing the FireCCI5.1 mean annual burn fraction with the HansenGFC-MAF mean annual burn fraction. Note: Percentage is shown on a log scale.*

Looking at the proportion of fires that are stand-replacing (Figure 3c), we find that in 40% of areas 100% of the observed fires were stand replacing, with an area weighted mean stand replacing fire percentage of 69% across the entire domain. The fraction of fires that are stand replacing varies considerably for each dominant tree species (Supplementary Figure 4). In the pine, larch and spruce forests, which dominate in the eastern half of the continent, the only fires detected were stand-replacing in more than 40% of areas, with only a small fraction of areas having a high proportion of non-stand-replacing fires. By contrast, Fir, Birch and Aspen, as well as the Maple, Linden, Beech and Oak which make up the *other* category, all have large proportions of their areas with low rates of stand replacing fires (Supplementary Figure 4).

3.3 Current risk of RF induced forest loss

In total there are 64 858 km^2 of forests that are at extreme risk of fire driven permanent forest loss, 92, 403 km^2 at high risk, 1.86 M km^2 at moderate risk, and 8.85 M km^2 at low risk based on the criteria outlined in section 2.4 and Table 2. The largest areas at high or extreme risk are found in the eastern half of the continent (Figure 4).

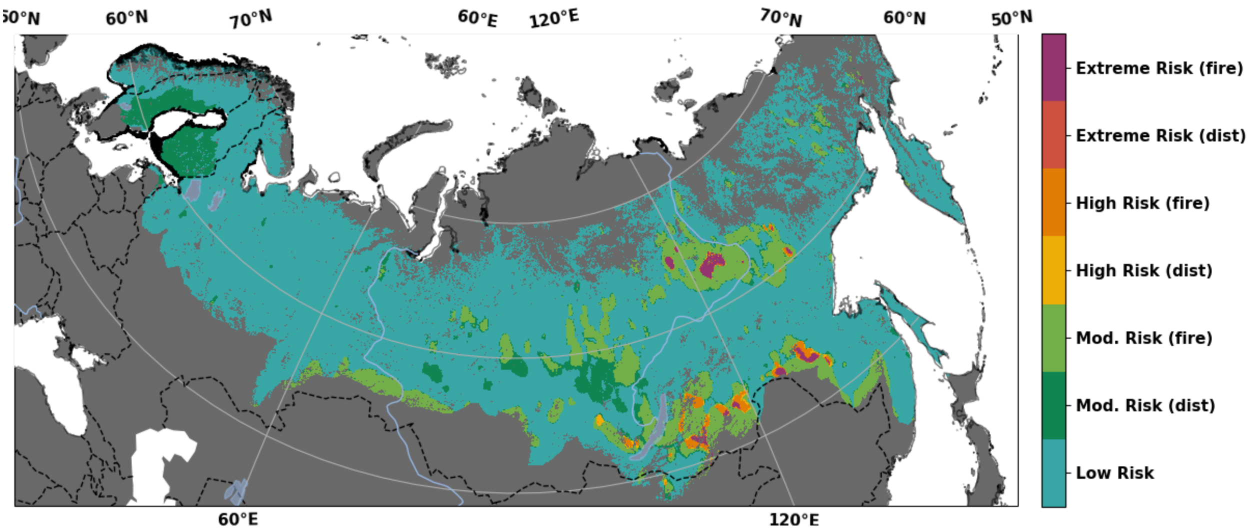

Figure 4 Current Risk of Forest Loss. *The risk of permanent forest loss using FRI, FRI_{SR} and DRI over the period 2001 to 2018. Criteria are shown in Table 2.*

3.4 FRI and Climatology

Over Eurasia the mean maximum monthly temperature decreases from south to north, while the mean annual rainfall shows a decrease from west to east (Figure 5a-b). The regions with the lowest mean annual rainfall are along the forest-steppe boundary as well as in Eastern Siberia. Broadly, this tracks with FRI estimates shown in Figure 2 with short FRI's found in hotter and drier areas. We find that between 1985 and 2015, climate change has driven a median increase in temperature over the

Eurasian Forest zone of 0.04°C per year, with the largest increases in temperature coming in winter and spring (Supplementary Figure 5). Interestingly, while the climate change-driven trends in precipitation are mixed, only regions with negative trends (Figure 5) are statistically significant (α_{FDR} = 0.10). This pattern holds when considering the seasonal trends as well which is shown in the seasonal breakdown of the trends and the climatology included in Supplementary Figure 5 and 6 respectively.

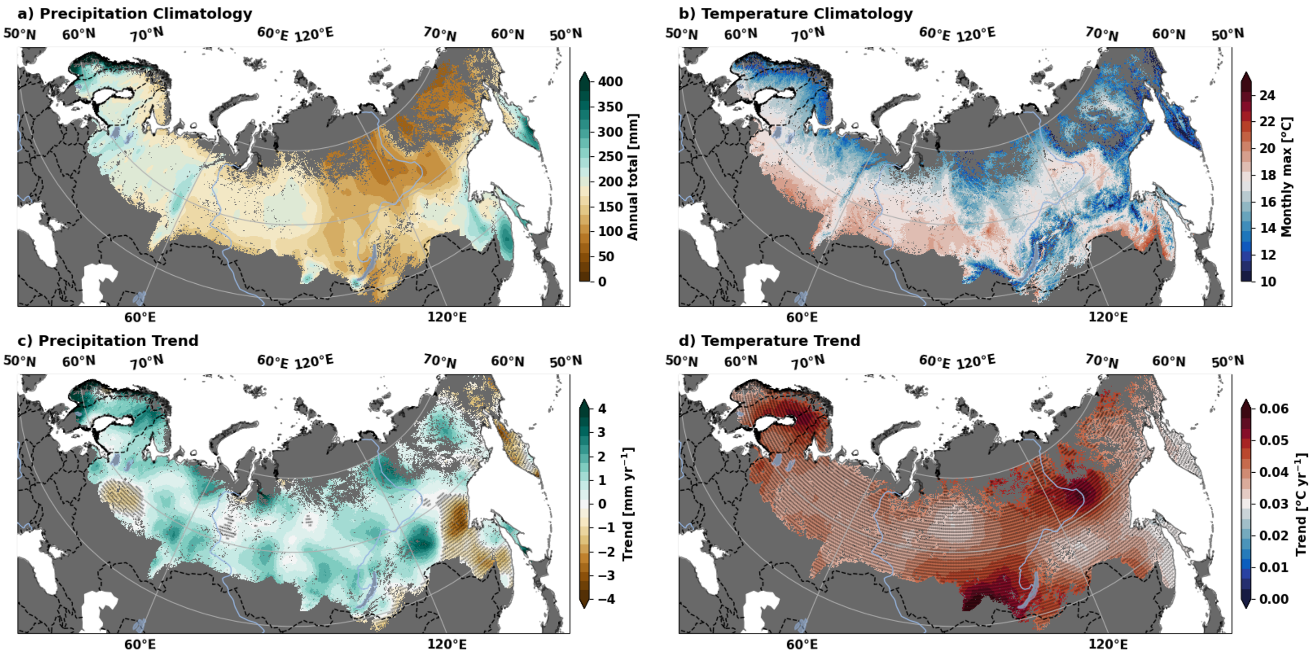

Figure 5 Climatology, climate trends and land cover. *Panels show a) the mean annual precipitation (1985 to 2015), b) the mean of the maximum monthly temperature (1985 to 2015), c) climate change-driven trend in mean annual precipitation (1985 to 2015), d) climate change-driven trend in the mean annual temperature (1985 to 2015). Non-boreal forest ecosystems are masked in grey, and, for panels c and d, the stippling indicates statistical significance (α_{FDR} = 0.10). Data: TerraClimate (Abatzoglou et al., 2018).*

Over the Eurasian boreal forest, there is a strong link between FRI and climatology, with the XGBoost ML regression models generated using the four BA datasets and seasonal climatology having an out of sample FRI R^2 of 0.60 for GFED4, 0.54 for MCD64A1, 0.53 for CGLS-BA and 0.47 for FireCCI51. Despite having the lowest overall R^2, the FireCCI51 model has the best skill when predicting areas with FRI < 60 years and is the only model to have any skill at predicting regions with an FRI of <15 years (Figure 6a-d). All models do well in the 30 to 60, 60 to 120, and the 120 to 500 years groups but have poor performance for all FRI's > 500. Overall, we find that temperature variables have more model importance than precipitation variables, with summer temperatures being the strongest explanatory variable (Figure 6).

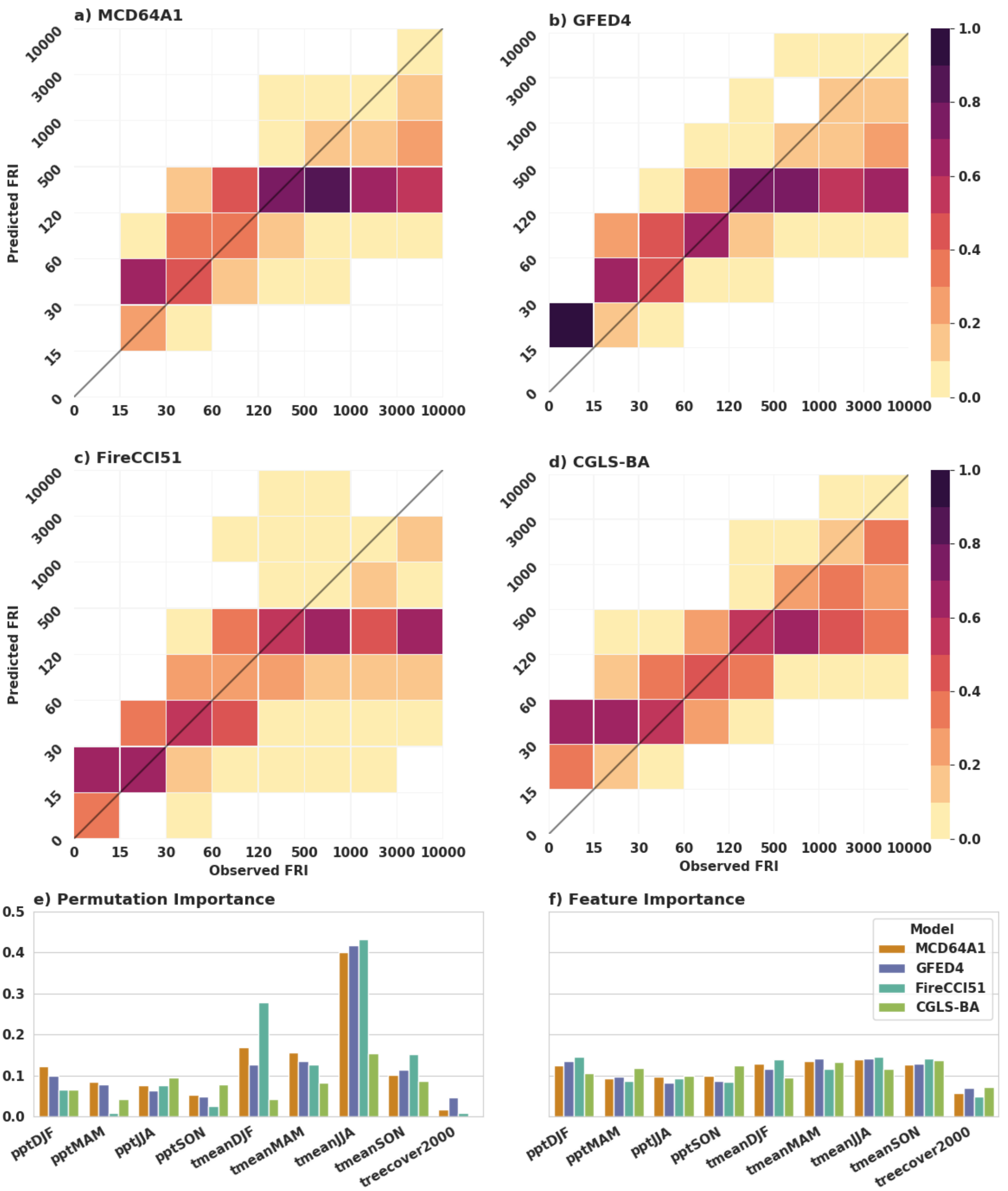

Figure 6 Modelling Landscape FRI using XGBoost. *Panels a-d show heatmaps of the observed FRI vs predicted FRI for four XGBoost models trained using a) GFED4, b) MCD64A1, c) FireCCI51, and d) CGLS-BA burned area data. The results have been binned using the same categories as Figure 2 and then normalised by dividing the number of points in the Observed FRI category so that each column sums to 1. The black line represents the 1 to 1 line where all values would fall in a perfect model. Panels e and f show the importance of different predictor variables determined using a e) Permutation Importance test, and f) Feature Importance test, where ppt is mean precipitation and tmean is mean temperature for the different meteorological seasons (DJF, MAM, JJA and SON) (Abatzoglou et al., 2018). treecover2000 is the fractional treecover in the year 2000 (Hansen et al., 2013).*

3.5 FRI under future climate condition

Using the XGBoost machine learning model fitted between FRI and observed climatology, applied to the five future climatology scenarios, we found that the climate change will drive a widespread shortening of the FRI over the next century (Figure 7). Given current trends in climatology and the FireCCI51 model, we find that areas with a modelled FRI <30 years will increase from 0.55 M km^2 over the observed period (1985-2015) (Figure 7a) to 2.99 M km^2 by the end of the century (2085 to 2115) (Figure 7d). This result also holds when our machine learning model is applied to the CMIP-5 based Terraclimate future climate dataset (TCfut) as shown in Figure 7e (2.64 M km^2 for 2085 to 2115). Both the trend and TCfut models show these increases occurring almost entirely in the coniferous forests of eastern Siberia, much of which is already at some level of permanent forest loss risk (Figure 4). This suggests that >25 % of all Eurasian boreal forests would be at high risk of fire-driven forest loss by the end of the century. We only report the results of the FireCCI model in this section because the models derived from other datasets could not reproduce FRI <30 years over the observed period in a fully withheld testing dataset (Figure 6). The results of the other BA dataset are shown in Supplementary Figure 7-9 and the results using multivariate linear regression instead of XGBoost are shown in Supplementary Figure 10-13.

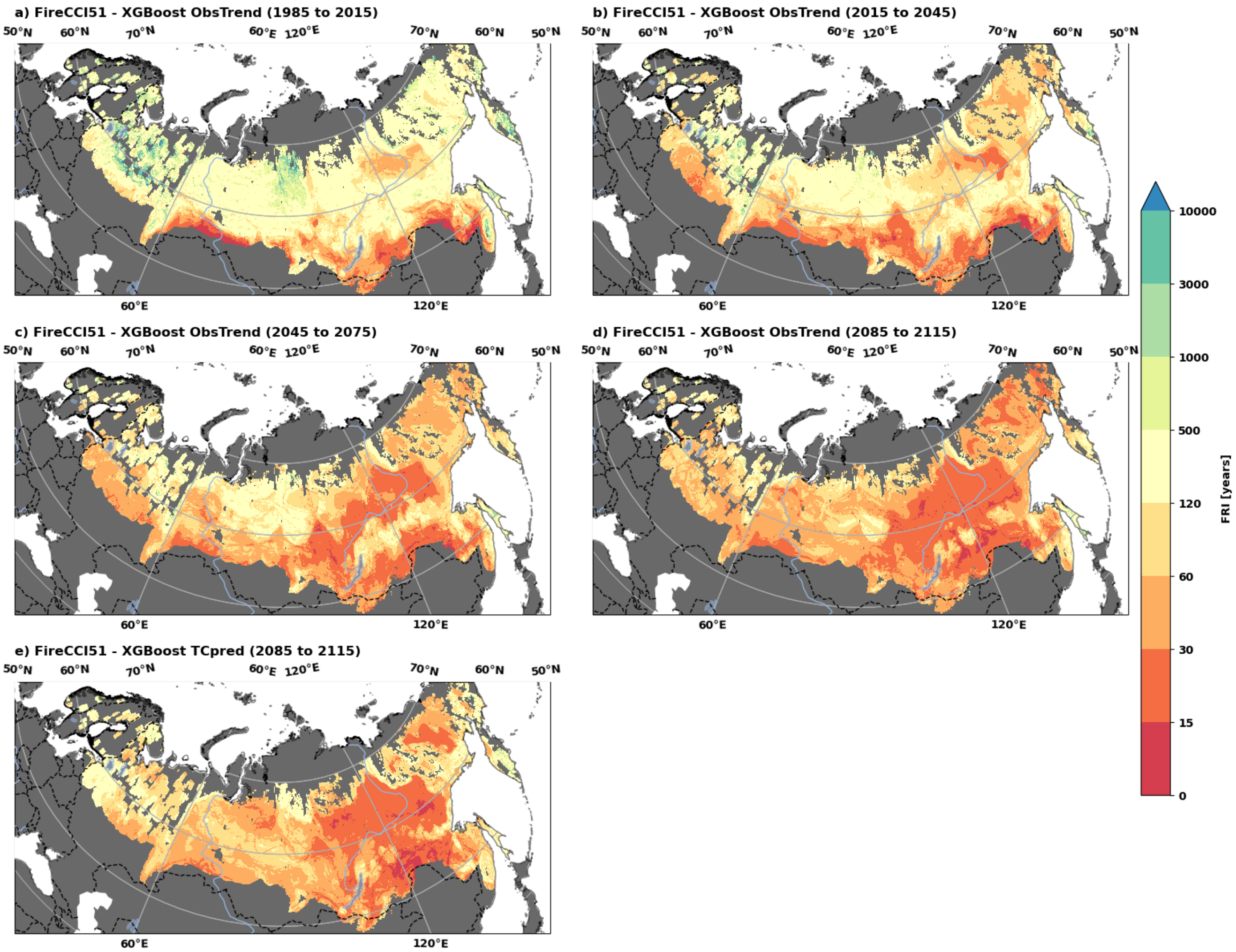

Figure 7 Maps of the predicted FRI *a-d) based on current climate trend, XGBoost and FireCCI51 FRI data. e) TCpred is the TerraClimate prediction for a 4⁰C warmer world, which approximates SSP3-7.0 2085 – 2115*

3.6 Future risk of RF induced forest loss

Using the future based estimate of FRI (Figure 7d) and the criteria outlined in section 2.4 to predict the future of RF induced forest loss, we find that the area at high or extreme risk will rise rapidly over the coming century with a 5 fold increase predicted from the 2015 to 2045 window compared to the 1985 to 2015 baseline (Table 3).

Table 3 Total areas at risk of RF induced forest loss over the next century. *TCpred refers to the future predictions that use the Terrclimate future climate dataset based on CMIP-5 models.*

	1985-2015	2015-2045	2045-2075	2085-2115	2085-2115 TCpred
Low Risk	9 096 172	6 774 806	5 268 266	4 140 387	4 992 808
Moderate risk	1 661 365	3 555 590	4 107 291	4 198 496	3 465 230
High Risk	53 098	158 719	185 048	199 835	140 234
Extreme Risk	48 078	369 593	1 298 134	2 320 026	2 260 526

Looking to the end of the century (2085 to 2115), we predict a 25-fold increase in high and extreme risk areas using a XGBoost model trained on trend based climate estimates and a 24-fold increase using the CMIP based Terraclimate future data. As shown in Figure 8, almost all of this increased risk is predicted to occur in the eastern half of the continent.

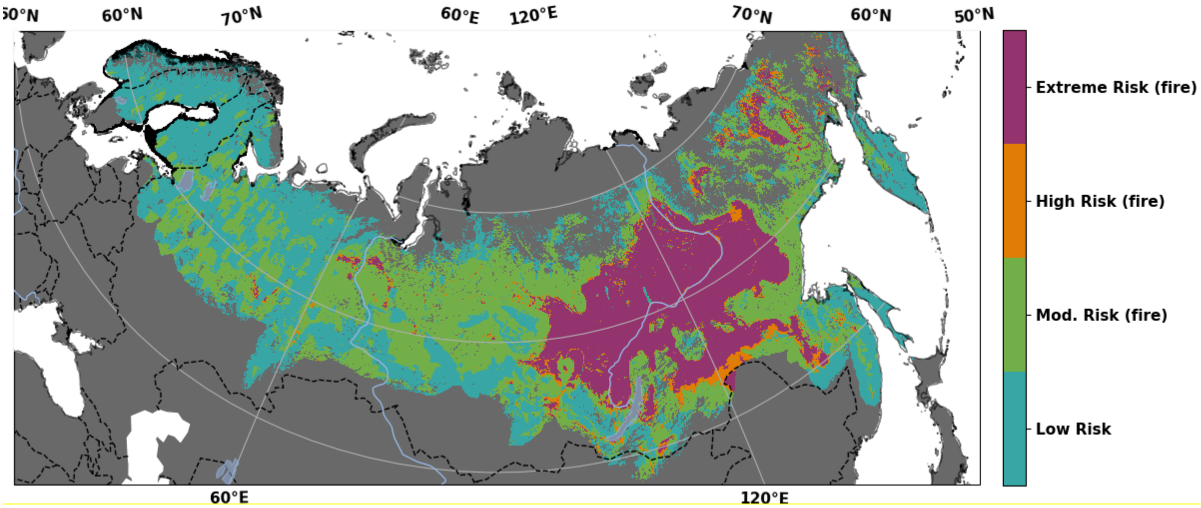

Figure 8 Risk of Forest Loss by 2085 to 2115. *The risk of permanent forest loss using future FRI estimated using XGBoost and FireCCI51, assuming that the fraction of fires that are stand-replacing remains constant through time. Criteria are shown in Table 2.*

4. Discussion

4.1 The patterns and drivers of the observed FRI

Broadly speaking, all datasets showed a shortening of the FRI from north to south and from west to east, which is consistent with previous research and fire ecology for the region (Kharuk et al., 2021; Kharuk and Ponomarev, 2017; Ponomarev et al., 2016). However, we find higher annual burn fractions and shorter FRI's than previous studies (Kharuk et al., 2021, 2016; Ponomarev et al., 2016) likely because of omission bias present in the AVHRR and MODIS BA datasets used in those studies (Humber et al., 2019; Lizundia-Loiola et al., 2020; Mouillot et al., 2014; Potapov et al., 2008). Both our accuracy assessment (Supplementary text 1.2) and larger assessments of BA accuracy suggest that, despite significant improvements in the recent versions of the MCD64A1 and FireCCI51, all BA datasets tested have a net omission bias because BA products often fail to identify small surface fires (Humber et al., 2019; Lizundia-Loiola et al., 2020). A recent high resolution regional study in Siberia found FRI's that were far shorter than had been previously reported (Sizov et al., 2021). This suggests that even FireCCI51, the dataset with the shortest median FRI, is likely underestimating the actual annual burned fraction.

The strong link between climatology and FRI over the Eurasian boreal zone shown in Figure 6 is consistent with previous studies that used both remotely sensed and paleo reconstructions of the fire dynamics and found that they are strongly associated with climatology (Feurdean et al., 2020; Forkel et al., 2012; Gaboriau et al., 2020; Kharuk et al., 2021; Kharuk and Ponomarev, 2017; Ponomarev et al., 2016). The summer temperature is the strongest predictor of landscape FRI (Figure 6), which is consistent with previous studies (Natole et al., 2021; Tomshin and Solovyev, 2021). This is alarming because most of eastern Eurasia is experiencing a summer warming rate of $>0.04^{o}$C per year (Supplementary Figure 2). The results of this study support previous findings that hotter and drier conditions are resulting in more frequent, and higher severity, fires (Feurdean et al., 2020; IPCC, 2021; Natole et al., 2021).

Looking at the proportion of stand replacing fires, Supplementary Figure 4 shows that the likelihood of a fire being stand replacing varies considerably with dominant tree species. In the larch and pine-dominated forests of Eastern Siberia (Bartalev et al., 2004), the DRI and FRI_{SR} are extremely consistent with each other and close to 100% of fires detected are stand replacing (Figure 3c and Supplementary Figure 4), which suggests that fire is the dominant driver of stand dynamics. This matches with the findings of previous studies that suggest Siberian conifer species such as *Pinus sylvestris* experience a FRI_{SR} of >~150 years (Feurdean et al., 2020). The stand-replacing fire percentage in these areas is higher than would be expected considering the prevalence of low stand mortality surface fires observed in previous studies that used AVHRR and MODIS BA data (Kharuk et al., 2021; Ponomarev et al., 2016). For example, Krylov et al. (2014) found that larch, pine and fir species have stand-replacing fire percentages in the 40 to 70% range. The discrepancy between our findings and existing studies can be explained by the BA omission bias discussed above and supports the conclusions that the BA products are omitting a large portion of the low stand mortality surface fires.

In contrast, forests in Western Siberia and in the Russian Far East along the Russia-China border north of Vladivostok, do not have a stand-replacing fire dynamic with stand-replacing fires making up <1% of BA (Figure 3c). In Western Siberia, the boreal and steppe biomes are separated by a strip of birch-dominated temperate continental forest (FAO, 2000; Feurdean et al., 2020). In these regions we find FRI_{SR} of >1000 years despite FRI's of <30 years. These findings are consistent with previous work that found short FRI's but very low stand mortality (Feurdean et al., 2020; Shuman et al., 2017) and suggest that these areas are at lower risk of permanent forest loss.

4.2 Current forest loss risk

In total, our framework for characterising the risk of RF induced permanent forest loss identified 155,261 km^2 of forests that are at high or extreme risk (Figure 4). When examining the Zabaikal region, located to the east of Lake Baikal near Chita in southern Siberia (Figure 5e), which is a known hotspot of post-fire recruitment failure (Barrett et al., 2020; Kukavskaya et al., 2016; Shvetsov et al., 2019), all MODIS-derived BA products have large areas with FRI's of <30 years as well as both DRI's and FRI_{SR}'s of <120 years. In this region the risk framework identifies large areas with high and extreme fire risk. This supports the use of this framework to identify other potential hotspots.

Similar patterns to the ones found in the Zabaikal region are apparent between Krasnoyarsk and Irkutsk, as well as in the forests west of Yakutsk. As such, these regions are probable hotspots of post-fire recruitment failure and forest loss. Field-based studies, most of which are published only in Russian, have found post-fire deforestation in the ribbon-like Scots pine forests grown in the zone of dry forest-steppe in the Altai region, Minusinsk stands of the Krasnoyarsk krai and the Balgazynsky pine forests of the Tyva Republic (Buryak et al., 2011; Ishutin, 2004; Kupriyanov et al., 2003; Paramonov and Ishutin, 1999). All three areas are found between Krasnoyarsk and the Russia-Mongolia border. At time of writing, the authors of this study are aware of no studies looking at postfire RF in Yakutia and the Far East.

In the Zabaikal and Yakutia regions, the risk framework shown in Figure 4 identified high or extreme disturbance-driven risk. The link between DRI and permanent forest loss is more nuanced than the link with FRI. When a short DRI is coincident with a short FRI, it can drive forest loss by increasing the *"resilience debt"* (Burrell et al., 2021; Johnstone et al., 2016). Previous studies have shown that repeat disturbances, especially post-fire salvage logging which is a common practice in many regions, contributes to recruitment failure in Siberia (Burrell et al., 2021; Kukavskaya et al., 2016). Logging can also replace the initial stand-replacing fire in the RF regime. In Russia, it is standard practice to replant trees after logging, but ~50% of the areas replanted in the most fire-prone parts of southern Siberia burn again within 15 years (Kukavskaya et al., 2016), which is likely to result in RF and forest loss. By contrast, in Scandinavia, where there is a <120 year DRI as the result of the widespread managed forestry (Curtis et al., 2018; Hansen et al., 2013) but a FRI of > 10,000 years, there is likely low risk of permanent forest loss. Interestingly, DRI's over central and western Eurasia are considerably shorter than the FRI_{SR}, which indicates forest loss is still prevalent, even if it is not being caused by fires (Figure 3b) (Curtis et al., 2018). Given this nuanced relationship, areas with a short FRI and short DRI's, but much longer FRI_{SR} (Mod. Risk and High Risk (dist) in Figure 3c), are arguably still at higher risk of forest loss and should be the focus of future research.

4.3 Future forest loss risk

Our modelling results predict that Eurasia will experience a large and consistent increase in the area with a predicted FRI <30 years throughout the next century as the earth warms (Figure 7) which has large impact of the risk of RF induced forest loss. We estimate that area of forest at high or extreme risk during the 2015 to 2045 window will grow to 530, 000 km^2, which is more than double the amount of area predicted for the 1985-2015 reference period. While no comparable estimates exists for comparison, both the 2020 and 2021 fire seasons, which are not included in the data used in this study, have been exceptionally large with some of the most extensive burns occurring in Yakutia (Ponomarev et al., 2021) where we predict large changes in FRI. Looking forward to the end of the century, both the trend-based and CMIP model-based estimates of future risk predict more than 2.5M km^2 (>20%) will have high or extreme risk of forest loss, with almost all of this increase in the risk of future fire-driven forest loss occurring over the pine and larch forests of Eastern Eurasia.

Current Earth System Models (ESMs), Land Surface Models, and even ecosystem-scale forest models, predict or assume gains or stability in the extent of boreal tree cover (Friend et al., 2014; Shuman et al., 2017). These models often underestimate the FRI (Shuman et al., 2017), if complex fire-vegetation interactions are modelled at all. There are only four models included in CMIP-6 that can model fire prognostically with future coupled projections (EC-Earth3-Veg, CESM2, CNRM-ESM2-1 and MPI-ESM1-2-LR) (Sanderson and Fisher, 2020). Even the state of the art fire models assessed in Fire Model Intercomparison Project use vegetation type as an input (Hantson et al., 2020) and are therefore not currently suited to modelling the possibility of fire-induced changes in vegetation type caused by post-fire RF. Currently, the best prediction of ecosystem change in the Eurasian boreal zone use Species Distribution Models (SDMs) in combination with ESMs to investigate changes in habitat suitability (Noce et al., 2019). This modelling approach predicts significant changes in the dominant species across Eurasia, but no major shift in the extent of forest zone itself. However, this approach does not consider fire and cannot account for post-fire RF (Noce et al., 2019). The most recent IPCC report, however, identified uncertainties around indirect CO_2 emissions from things like forest fires as a key limitation that can greatly impact our ability to predict the changes that will occur over the next 100 years (IPCC, 2021) suggesting an urgent need for coupled climate vegetation models including realistic disturbance dynamics.

Eastern Eurasia contains some of the largest areas of unmanaged primary forest in the world (Potapov et al., 2017) and the widespread loss of forest in this region will accelerate the loss of habitats and associated biodiversity that is already occurring at an alarming rate (Brondizio et al., 2019; Dinerstein et al., 2017). The Eurasian boreal zone contains globally significant amounts of carbon stored in both the above ground biomass and the soil (Brondizio et al., 2019; Kharuk et al., 2021). Previous studies have shown that increases in the frequency of fires will drive widespread carbon loss and amplify the impacts of climate change (de Groot et al., 2013; Kharuk et al., 2021). In addition to the global impacts, an increase in fire frequency will likely worsen air quality problems and associated health issues that already occur in cities like Novosibirsk, Krasnoyarsk and Yakutsk during large fire years (Kharuk et al., 2021). The loss of forest goods and commercially valuable tree species is likely to negatively impact upon the economic and social well-being of the local population which is reliant on the forestry industry (Leskinen et al., 2020) and could contribute to the further loss of indigenous culture and language in the region (Brondizio et al., 2019).

4.4 The limitations of future predictions of forest loss

The main limitation of our FRI prediction approach is that we are unable to consider secondary effects and feedback loops. For example, increases in drought severity and summer temperatures may lead to a large increase in the portion of fires that are stand-replacing (de Groot et al., 2013; Tepley et al., 2018). At the same time, heatwave and drought events which are increasing with climate change are potentially greatly reducing the survivability of seedling and saplings (Boucher et al., 2019; Sannikov et al., 2020). Our modelling approach assumes a constant tree cover, but there is strong evidence that forest fragmentation results in an increase in the frequency of fires as a result of increased human access which lead to significantly more ignitions (Driscoll et al., 2021; Shvetsov et al., 2021), as well as forest edge effects that increase the flammability of the forest (Driscoll et al., 2021). Also, our approach does not consider distance to seed source which is an important predictor of recruitment failure in many regions, with sites adjacent to mature forest having a lower risk of RF (Hansen et al., 2018). However, we expect that this will not significantly change our risk categorisation because we considered dynamics at a spatial scale 3 to 4 orders of magnitude larger than the distance over which seed sources can offer a protective effect (Hansen et al., 2018). Areas with higher or extreme risk experience stand replacing fires and forest fragmentation at a scale that will greatly limit the protective effect of adjacent seed sources, though further research on this point is needed.

One feedback loop that might act to mitigate the risk of fire induced forest loss is the species balance shift from conifers to broadleaf tree species such as trembling aspen (*Populus tremuloides*) (Gill et al., 2017; Johnstone and Chapin, 2006; Whitman et al., 2019). This transition has been widely observed in boreal North America (Gill et al., 2017; Johnstone and Chapin, 2006; Whitman et al., 2019), and has been described as a potential strategy to mitigate the impact of an increase in forest fires (Astrup et al., 2018). Whilst this dynamic has also been observed in Eurasia (Kharuk et al., 2021), it is highly unlikely to be able to offset the forest loss predicted by this study. In Eurasia, temperature, and to a lesser extent, water availability, is the key limiting factor in reshaping species ranges (Noce et al., 2019). This means that while models currently predict a significant expansion in the range of Aspen throughout this century (Noce et al., 2019), almost all this expansion is predicted to occur in western Eurasia, with almost none occurring in areas where we predict fire-induced forest loss risk increases. Another feedback loop that might act to mitigate the risk of fire induced forest loss is that increased burning may have a long-term negative feedback on fire frequency because of reductions in fuel availability (Bernier et al., 2016), though evidence from throughout the boreal zone suggests that the effect can be completely offset by the establishment of flammable grasses (Kukavskaya et al., 2014; Stralberg et al., 2018).

When the potential increase in stand-replacing fires (de Groot et al., 2013; Tepley et al., 2018), the reduced survivability of seedlings (Boucher et al., 2019; Sannikov et al., 2020) and the increase in fire frequency (Driscoll et al., 2021; Kukavskaya et al., 2014) are considered together, a strong likelihood of a positive feedback mechanism emerges which, in turn, raises the concerning possibility that the predictions shown in Figure 7 may actually underestimate the risk of future fire driven RF induced forest loss. Unlike boreal North America, species balance shifts are much less likely to mitigate the risk of increased fires.

5. Conclusions

Understanding the processes that may drive significant changes to the extent of the boreal forest biome is essential for understanding the impacts of climate change on the biosphere and feedbacks to future climate change (Kharuk et al., 2021). Our results show that 1.2 % of the Eurasian boreal zone is already at high or extreme risk of fire induced forest loss with a further 11 % of areas at moderate risk. Given current warming rates, >20 % of the Eurasian forest zone is likely to be at high risk by the end of the century. This poses a substantial risk to the forestry industry in the region and has the potential to dampen, and potentially, even reverse, the boreal carbon sink. As such, there is an urgent need for more research to examine this critical dynamic in the field and to include it in models of vegetation and climate feedbacks.

6. Acknowledgments

This work was supported by (i) the UK Natural Environment Research Council [grant number NE/N009495/1] awarded to KB, RB and JK and (ii) the National Aeronautics and Space Administration (NASA) Arctic Boreal Vulnerability Experiment (ABoVE) grant 80NSSC19M0112. EK and SZ acknowledge funding support from the RFBR, Government of the Krasnoyarsk krai and the Krasnoyarsk Regional Foundation of Scientific and Scientific-Technical Support (Grant #20-44-242004).

7. Author contributions

ALB and KB conceived the study. ALB developed the methodology with input from KB, RB and QS. ALB performed the analysis and wrote the manuscript with input from QS, RB, EAK, SZ, TS, BMR, JK and KB.

8. Data Availability

All datasets used in this study are publicly available and can be accessed from their original creators.

9. Code availability

The code will be made available upon publication.

10. References

Abatzoglou, J.T., Dobrowski, S.Z., Parks, S.A., Hegewisch, K.C., 2018. TerraClimate, a high-resolution global dataset of monthly climate and climatic water balance from 1958–2015. Sci. Data 5, 170191. https://doi.org/10.1038/sdata.2017.191

Abdelmoaty, H.M., Papalexiou, S.M., Rajulapati, C.R., AghaKouchak, A., 2021. Biases Beyond the Mean in CMIP6 Extreme Precipitation: A Global Investigation. Earths Future 9, e2021EF002196. https://doi.org/10.1029/2021EF002196

Abram, N.J., Wright, N.M., Ellis, B., Dixon, B.C., Wurtzel, J.B., England, M.H., Ummenhofer, C.C., Philibosian, B., Cahyarini, S.Y., Yu, T.-L., Shen, C.-C., Cheng, H., Edwards, R.L., Heslop, D., 2020. Coupling of Indo-Pacific climate variability over the last millennium. Nature 579, 385–392. https://doi.org/10.1038/s41586-020-2084-4

Ahmed, K., Shahid, S., Nawaz, N., 2018. Impacts of climate variability and change on seasonal drought characteristics of Pakistan. Atmospheric Res. 214, 364–374. https://doi.org/10.1016/j.atmosres.2018.08.020

Akinsanola, A.A., Kooperman, G.J., Reed, K.A., Pendergrass, A.G., Hannah, W.M., 2020. Projected changes in seasonal precipitation extremes over the United States in CMIP6 simulations. Environ. Res. Lett. 15, 104078. https://doi.org/10.1088/1748-9326/abb397

Archibald, S., Lehmann, C.E.R., Gómez-Dans, J.L., Bradstock, R.A., 2013. Defining pyromes and global syndromes of fire regimes. Proc. Natl. Acad. Sci. 201211466. https://doi.org/10.1073/pnas.1211466110

Astrup, R., Bernier, P.Y., Genet, H., Lutz, D.A., Bright, R.M., 2018. A sensible climate solution for the boreal forest. Nat. Clim. Change 8, 11–12. https://doi.org/10.1038/s41558-017-0043-3

Baltzer, J.L., Day, N.J., Walker, X.J., Greene, D., Mack, M.C., Alexander, H.D., Arseneault, D., Barnes, J., Bergeron, Y., Boucher, Y., Bourgeau-Chavez, L., Brown, C.D., Carrière, S., Howard, B.K., Gauthier, S., Parisien, M.-A., Reid, K.A., Rogers, B.M., Roland, C., Sirois, L., Stehn, S., Thompson, D.K., Turetsky, M.R., Veraverbeke, S., Whitman, E., Yang, J., Johnstone, J.F., 2021. Increasing fire and the decline of fire adapted black spruce in the boreal forest. Proc. Natl. Acad. Sci. 118. https://doi.org/10.1073/pnas.2024872118

Barrett, K., Baxter, R., Kukavskaya, E., Balzter, H., Shvetsov, E., Buryak, L., 2020. Postfire recruitment failure in Scots pine forests of southern Siberia. Remote Sens. Environ. 237, 111539. https://doi.org/10.1016/j.rse.2019.111539

Bartalev, S., Yaroshenko, A., Ershov, D., A.S., I., Potapov, P., Turubanova, S., 2004. Russia’s Forests Dominating Forest Types and Their Canopy Density.

Bartholomé, E., Belward, A.S., 2005. GLC2000: a new approach to global land cover mapping from Earth observation data. Int. J. Remote Sens. 26, 1959–1977. https://doi.org/10.1080/01431160412331291297

Bernier, P.Y., Gauthier, S., Jean, P.-O., Manka, F., Boulanger, Y., Beaudoin, A., Guindon, L., 2016. Mapping Local Effects of Forest Properties on Fire Risk across Canada. Forests 7, 157. https://doi.org/10.3390/f7080157

Beverly, J.L., 2017. Time since prior wildfire affects subsequent fire containment in black spruce. Int. J. Wildland Fire 26, 919–929. https://doi.org/10.1071/WF17051

Bläsche, T., Bowden, R.J., Posch, P.N., 2014. Data smoothing and end correction using entropic kernel compression. Stat 3, 250–257. https://doi.org/10.1002/sta4.59

Boucher, D., Gauthier, S., Thiffault, N., Marchand, W., Girardin, M., Urli, M., 2019. How climate change might affect tree regeneration following fire at northern latitudes: a review. New For. https://doi.org/10.1007/s11056-019-09745-6

Bradshaw, C.J.A., Warkentin, I.G., 2015. Global estimates of boreal forest carbon stocks and flux. Glob. Planet. Change 128, 24–30. https://doi.org/10.1016/j.gloplacha.2015.02.004

Brazhnik, K., Hanley, C., Shugart, H.H., 2017. Simulating Changes in Fires and Ecology of the 21st Century Eurasian Boreal Forests of Siberia. Forests 8, 49. https://doi.org/10.3390/f8020049

Brennan, J., Gómez-Dans, J.L., Disney, M., Lewis, P., 2019. Theoretical uncertainties for global satellite-derived burned area estimates. Biogeosciences 16, 3147–3164. https://doi.org/10.5194/bg-16-3147-2019

Brodie, J.F., Roland, C.A., Stehn, S.E., Smirnova, E., 2019. Variability in the expansion of trees and shrubs in boreal Alaska. Ecology e02660. https://doi.org/10.1002/ecy.2660

Brondizio, E.S., Settele, J., Díaz, S., Ngo, H.T., 2019. Global assessment report on biodiversity and ecosystem services of the Intergovernmental Science-Policy Platform on Biodiversity and Ecosystem Services. IPBES Secr. Bonn.

Broome, A., Summers, R.W., Vanhala, T., 2016. Understanding the provision of conifer seed for woodland species. Res. Note-For. Comm.

Brown, C.D., Johnstone, J.F., 2012. Once burned, twice shy: Repeat fires reduce seed availability and alter substrate constraints on Picea mariana regeneration. For. Ecol. Manag. 266, 34–41. https://doi.org/10.1016/j.foreco.2011.11.006

Burrell, A.L., Evans, J.P., De Kauwe, M.G., 2020. Anthropogenic climate change has driven over 5 million km 2 of drylands towards desertification. Nat. Commun. 11, 3853. https://doi.org/10.1038/s41467-020-17710-7

Burrell, A.L., Evans, J.P., Liu, Y., 2019. The Addition of Temperature to the TSS-RESTREND Methodology Significantly Improves the Detection of Dryland Degradation. IEEE J. Sel. Top. Appl. Earth Obs. Remote Sens. 1–7. https://doi.org/10.1109/JSTARS.2019.2906466

Burrell, A.L., Kukavskaya, E.A., Baxter, R., Sun, Q., Barrett, K., 2021. Post-fire recruitment failure as a driver of forest to non-forest ecosystem shifts in boreal regions, in: Ecosystem Collapse and Climate Change, Ecological Studies. Springer International Publishing.

Buryak, L.V., Sukhinin, A.I., Kalenskaya, O.P., Ponomarev, E.I., 2011. Effects of fires in ribbon-like pine forests of southern Siberia. Contemp. Probl. Ecol. 4, 248–253. https://doi.org/10.1134/S1995425511030039

Cai, W.H., Liu, Z., Yang, Y.Z., Yang, J., 2018. Does Environment Filtering or Seed Limitation Determine Post-fire Forest Recovery Patterns in Boreal Larch Forests? Front. Plant Sci. 9. https://doi.org/10.3389/fpls.2018.01318

Chen, D., Dai, A., Hall, A., 2021. The Convective-To-Total Precipitation Ratio and the "Drizzling" Bias in Climate Models. J. Geophys. Res. Atmospheres 126, e2020JD034198. https://doi.org/10.1029/2020JD034198

Chen, D., Loboda, T.V., 2018. Surface forcing of non-stand-replacing fires in Siberian larch forests. Environ. Res. Lett. 13, 045008. https://doi.org/10.1088/1748-9326/aab443

Chen, H.Y.H., Luo, Y., Reich, P.B., Searle, E.B., Biswas, S.R., 2016. Climate change-associated trends in net biomass change are age dependent in western boreal forests of Canada. Ecol. Lett. 19, 1150–1158. https://doi.org/10.1111/ele.12653

Chen, T., Guestrin, C., 2016. XGBoost: A Scalable Tree Boosting System. Proc. 22nd ACM SIGKDD Int. Conf. Knowl. Discov. Data Min. 785–794. https://doi.org/10.1145/2939672.2939785

Chmura, D.J., Rożkowski, R., Chałupka, W., 2012. Growth and phenology variation in progeny of Scots pine seed orchards and commercial seed stands. Eur. J. For. Res. 131, 1229–1243. https://doi.org/10.1007/s10342-012-0594-9

Chu, T., Guo, X., 2014. Remote Sensing Techniques in Monitoring Post-Fire Effects and Patterns of Forest Recovery in Boreal Forest Regions: A Review. Remote Sens. 6, 470–520. https://doi.org/10.3390/rs6010470

Coops, N.C., Hermosilla, T., Wulder, M.A., White, J.C., Bolton, D.K., 2018. A thirty year, fine-scale, characterization of area burned in Canadian forests shows evidence of regionally increasing trends in the last decade. PLOS ONE 13, e0197218. https://doi.org/10.1371/journal.pone.0197218

Coppola, E., Raffaele, F., Giorgi, F., Giuliani, G., Xuejie, G., Ciarlo, J.M., Sines, T.R., Torres-Alavez, J.A., Das, S., di Sante, F., Pichelli, E., Glazer, R., Müller, S.K., Abba Omar, S., Ashfaq, M., Bukovsky, M., Im, E.-S., Jacob, D., Teichmann, C., Remedio, A., Remke, T., Kriegsmann, A., Bülow, K., Weber, T., Buntemeyer, L., Sieck, K., Rechid, D., 2021. Climate hazard indices projections based on CORDEX-CORE, CMIP5 and CMIP6 ensemble. Clim. Dyn. 57, 1293–1383. https://doi.org/10.1007/s00382-021-05640-z

Curtis, P.G., Slay, C.M., Harris, N.L., Tyukavina, A., Hansen, M.C., 2018. Classifying drivers of global forest loss. Science 361, 1108–1111. https://doi.org/10.1126/science.aau3445

de Groot, W.J., Cantin, A.S., Flannigan, M.D., Soja, A.J., Gowman, L.M., Newbery, A., 2013. A comparison of Canadian and Russian boreal forest fire regimes. For. Ecol. Manag., The Mega-fire reality 294, 23–34. https://doi.org/10.1016/j.foreco.2012.07.033

Dinerstein, E., Olson, D., Joshi, A., Vynne, C., Burgess, N.D., Wikramanayake, E., Hahn, N., Palminteri, S., Hedao, P., Noss, R., Hansen, M., Locke, H., Ellis, E.C., Jones, B., Barber, C.V., Hayes, R., Kormos, C., Martin, V., Crist, E., Sechrest, W., Price, L., Baillie, J.E.M., Weeden, D., Suckling, K., Davis, C., Sizer, N., Moore, R., Thau, D., Birch, T., Potapov, P., Turubanova, S., Tyukavina, A., de Souza, N., Pintea, L., Brito, J.C., Llewellyn, O.A., Miller, A.G., Patzelt, A., Ghazanfar, S.A., Timberlake, J., Klöser, H., Shennan-Farpón, Y., Kindt, R., Lillesø, J.-P.B., van Breugel, P., Graudal, L., Voge, M., Al-Shammari, K.F., Saleem, M., 2017. An Ecoregion-Based Approach to Protecting Half the Terrestrial Realm. BioScience 67, 534–545. https://doi.org/10.1093/biosci/bix014

D'Orangeville, L., Houle, D., Duchesne, L., Phillips, R.P., Bergeron, Y., Kneeshaw, D., 2018. Beneficial effects of climate warming on boreal tree growth may be transitory. Nat. Commun. 9, 3213. https://doi.org/10.1038/s41467-018-05705-4

Driscoll, D.A., Armenteras, D., Bennett, A.F., Brotons, L., Clarke, M.F., Doherty, T.S., Haslem, A., Kelly, L.T., Sato, C.F., Sitters, H., Aquilué, N., Bell, K., Chadid, M., Duane, A., Meza-Elizalde, M.C., Giljohann, K.M., González, T.M., Jambhekar, R., Lazzari, J., Morán-Ordóñez, A., Wevill, T., 2021. How fire interacts with habitat loss and fragmentation. Biol. Rev. 96, 976–998. https://doi.org/10.1111/brv.12687

Edwards, C., Mason, W., 2006. Stand structure and dynamics of four native Scots pine (Pinus sylvestris L.) woodlands in northern Scotland. For. Int. J. For. Res. 79, 261–277. https://doi.org/10.1093/forestry/cpl014

Erni, S., Arseneault, D., Parisien, M.-A., 2018. Stand Age Influence on Potential Wildfire Ignition and Spread in the Boreal Forest of Northeastern Canada. Ecosystems 21, 1471–1486. https://doi.org/10.1007/s10021-018-0235-3

Falk, D.A., Miller, C., McKenzie, D., Black, A.E., 2007. Cross-Scale Analysis of Fire Regimes. Ecosystems 10, 809–823. https://doi.org/10.1007/s10021-007-9070-7

FAO, 2000. Global Forest Resources Assessment 2000: Main Reports (FAO Forestry Paper No. 140). UN Food and Agriculture Organization, Rome.

Feurdean, A., Florescu, G., Tanţău, I., Vannière, B., Diaconu, A.-C., Pfeiffer, M., Warren, D., Hutchinson, S.M., Gorina, N., Gałka, M., Kirpotin, S., 2020. Recent fire regime in the southern boreal forests of western Siberia is unprecedented in the last five millennia. Quat. Sci. Rev. 244, 106495. https://doi.org/10.1016/j.quascirev.2020.106495

Forbes, B.C., Fauria, M.M., Zetterberg, P., 2010. Russian Arctic warming and 'greening' are closely tracked by tundra shrub willows. Glob. Change Biol. 16, 1542–1554. https://doi.org/10.1111/j.1365-2486.2009.02047.x

Forkel, M., Thonicke, K., Beer, C., Cramer, W., Bartalev, S., Schmullius, C., 2012. Extreme fire events are related to previous-year surface moisture conditions in permafrost-underlain larch forests of Siberia. Environ. Res. Lett. 7, 044021. https://doi.org/10.1088/1748-9326/7/4/044021

Frazier, R.J., Coops, N.C., Wulder, M.A., Hermosilla, T., White, J.C., 2018. Analyzing spatial and temporal variability in short-term rates of post-fire vegetation return from Landsat time series. Remote Sens. Environ. 205, 32–45. https://doi.org/10.1016/j.rse.2017.11.007

Friend, A.D., Lucht, W., Rademacher, T.T., Keribin, R., Betts, R., Cadule, P., Ciais, P., Clark, D.B., Dankers, R., Falloon, P.D., Ito, A., Kahana, R., Kleidon, A., Lomas, M.R., Nishina, K., Ostberg, S., Pavlick, R., Peylin, P., Schaphoff, S., Vuichard, N., Warszawski, L., Wiltshire, A., Woodward, F.I., 2014. Carbon residence time dominates uncertainty in terrestrial vegetation responses to future climate and atmospheric CO2. Proc. Natl. Acad. Sci. 111, 3280–3285. https://doi.org/10.1073/pnas.1222477110

Gaboriau, D.M., Remy, C.C., Girardin, M.P., Asselin, H., Hély, C., Bergeron, Y., Ali, A.A., 2020. Temperature and fuel availability control fire size/severity in the boreal forest of central

Northwest Territories, Canada. Quat. Sci. Rev. 250, 106697. https://doi.org/10.1016/j.quascirev.2020.106697

Gauthier, S., Bernier, P., Kuuluvainen, T., Shvidenko, A.Z., Schepaschenko, D.G., 2015. Boreal forest health and global change. Science 349, 819–822. https://doi.org/10.1126/science.aaa9092

Giglio, L., Boschetti, L., Roy, D.P., Humber, M.L., Justice, C.O., 2018. The Collection 6 MODIS burned area mapping algorithm and product. Remote Sens. Environ. 217, 72–85. https://doi.org/10.1016/j.rse.2018.08.005

Gill, N.S., Sangermano, F., Buma, B., Kulakowski, D., 2017. Populus tremuloides seedling establishment: An underexplored vector for forest type conversion after multiple disturbances. For. Ecol. Manag. 404, 156–164. https://doi.org/10.1016/j.foreco.2017.08.008

Goetz, S.J., Bunn, A.G., Fiske, G.J., Houghton, R.A., 2005. Satellite-observed photosynthetic trends across boreal North America associated with climate and fire disturbance. Proc. Natl. Acad. Sci. 102, 13521–13525. https://doi.org/10.1073/pnas.0506179102

Guay, K.C., Beck, P.S.A., Berner, L.T., Goetz, S.J., Baccini, A., Buermann, W., 2014. Vegetation productivity patterns at high northern latitudes: a multi-sensor satellite data assessment. Glob. Change Biol. 20, 3147–3158. https://doi.org/10.1111/gcb.12647

Hansen, M.C., Potapov, P.V., Moore, R., Hancher, M., Turubanova, S.A., Tyukavina, A., Thau, D., Stehman, S.V., Goetz, S.J., Loveland, T.R., Kommareddy, A., Egorov, A., Chini, L., Justice, C.O., Townshend, J.R.G., 2013. High-Resolution Global Maps of 21st-Century Forest Cover Change. Science 342, 850–853. https://doi.org/10.1126/science.1244693

Hansen, W.D., Braziunas, K.H., Rammer, W., Seidl, R., Turner, M.G., 2018. It takes a few to tango: changing climate and fire regimes can cause regeneration failure of two subalpine conifers. Ecology 99, 966–977. https://doi.org/10.1002/ecy.2181

Hantson, S., Kelley, D.I., Arneth, A., Harrison, S.P., Archibald, S., Bachelet, D., Forrest, M., Hickler, T., Lasslop, G., Li, F., Mangeon, S., Melton, J.R., Nieradzik, L., Rabin, S.S., Prentice, I.C., Sheehan, T., Sitch, S., Teckentrup, L., Voulgarakis, A., Yue, C., 2020. Quantitative assessment of fire and vegetation properties in simulations with fire-enabled vegetation models from the Fire Model Intercomparison Project. Geosci. Model Dev. 13, 3299–3318. https://doi.org/10.5194/gmd-13-3299-2020

Hayes, D.J., McGuire, A.D., Kicklighter, D.W., Gurney, K.R., Burnside, T.J., Melillo, J.M., 2011. Is the northern high-latitude land-based CO2 sink weakening? Glob. Biogeochem. Cycles 25. https://doi.org/10.1029/2010GB003813

Huang, J., Tardif, J.C., Bergeron, Y., Denneler, B., Berninger, F., Girardin, M.P., 2010. Radial growth response of four dominant boreal tree species to climate along a latitudinal gradient in the eastern Canadian boreal forest. Glob. Change Biol. 16, 711–731. https://doi.org/10.1111/j.1365-2486.2009.01990.x

Humber, M.L., Boschetti, L., Giglio, L., Justice, C.O., 2019. Spatial and temporal intercomparison of four global burned area products. Int. J. Digit. Earth 12, 460–484. https://doi.org/10.1080/17538947.2018.1433727

IPCC, 2021. Climate Change 2021: The Physical Science Basis. Contribution of Working Group I to the Sixth Assessment Report of the Intergovernmental Panel on Climate Change.

Ishutin, Ya.N., 2004. Reforestation of Burned Areas in Ribbon-Like Pine Forest of Altai (Barnaul, 2004) [in Russian].

Johnstone, J.F., Allen, C.D., Franklin, J.F., Frelich, L.E., Harvey, B.J., Higuera, P.E., Mack, M.C., Meentemeyer, R.K., Metz, M.R., Perry, G.L., Schoennagel, T., Turner, M.G., 2016. Changing disturbance regimes, ecological memory, and forest resilience. Front. Ecol. Environ. 14, 369–378. https://doi.org/10.1002/fee.1311

Johnstone, J.F., Chapin, F.S., 2006. Effects of Soil Burn Severity on Post-Fire Tree Recruitment in Boreal Forest. Ecosystems 9, 14–31. https://doi.org/10.1007/s10021-004-0042-x

Johnstone, J.F., Hollingsworth, T.N., Chapin, F.S., Mack, M.C., 2010. Changes in fire regime break the legacy lock on successional trajectories in Alaskan boreal forest. Glob. Change Biol. 16, 1281–1295. https://doi.org/10.1111/j.1365-2486.2009.02051.x

Kauppi, P.E., Posch, M., Pirinen, P., 2014. Large Impacts of Climatic Warming on Growth of Boreal Forests since 1960. PLOS ONE 9, e111340. https://doi.org/10.1371/journal.pone.0111340

Keenan, T.F., Riley, W.J., 2018. Greening of the land surface in the world’s cold regions consistent with recent warming. Nat. Clim. Change 1. https://doi.org/10.1038/s41558-018-0258-y

Kharuk, V.I., Dvinskaya, M.L., Petrov, I.A., Im, S.T., Ranson, K.J., 2016. Larch forests of Middle Siberia: long-term trends in fire return intervals. Reg. Environ. Change 16, 2389–2397. https://doi.org/10.1007/s10113-016-0964-9

Kharuk, V.I., Ponomarev, E.I., 2017. Spatiotemporal characteristics of wildfire frequency and relative area burned in larch-dominated forests of Central Siberia. Russ. J. Ecol. 48, 507–512. https://doi.org/10.1134/S1067413617060042

Kharuk, V.I., Ponomarev, E.I., Ivanova, G.A., Dvinskaya, M.L., Coogan, S.C.P., Flannigan, M.D., 2021. Wildfires in the Siberian taiga. Ambio. https://doi.org/10.1007/s13280-020-01490-x

Koven, C.D., 2013. Boreal carbon loss due to poleward shift in low-carbon ecosystems. Nat. Geosci. 6, 452–456. https://doi.org/10.1038/ngeo1801

Krylov, A., McCarty, J.L., Potapov, P., Loboda, T., Tyukavina, A., Turubanova, S., Hansen, M.C., 2014. Remote sensing estimates of stand-replacement fires in Russia, 2002–2011. Environ. Res. Lett. 9, 105007. https://doi.org/10.1088/1748-9326/9/10/105007

Kukavskaya, E.A., Buryak, L.V., Shvetsov, E.G., Conard, S.G., Kalenskaya, O.P., 2016. The impact of increasing fire frequency on forest transformations in southern Siberia. For. Ecol. Manag. 382, 225–235. https://doi.org/10.1016/j.foreco.2016.10.015

Kukavskaya, E.A., Ivanova, G.A., Conard, S.G., McRae, D.J., Ivanov, V.A., 2014. Biomass dynamics of central Siberian Scots pine forests following surface fires of varying severity. Int. J. Wildland Fire 23, 872–886. https://doi.org/10.1071/WF13043

Kupriyanov, A.N., Trofimov, I.T., Zablotskiy, V.I., Makarychev, S.V., Kudryashov, I.V., Malinovskikh, A.A., Burmistrov, M.V., Strakowski, A.N., Bolotov, A.G., Begovich, Y., 2003. Restoration of forest ecosystems after fires.

Leskinen, P., Lindner, M., Verkerk, P.J., Nabuurs, G.-J., Van Brusselen, J., Kulikova, E., Hassegawa, M., Lerink, B. (Eds.), 2020. Russian forests and climate change, What Science Can Tell Us. European Forest Institute. https://doi.org/10.36333/wsctu11

Lin, X., Rogers, B.M., Sweeney, C., Chevallier, F., Arshinov, M., Dlugokencky, E., Machida, T., Sasakawa, M., Tans, P., Keppel-Aleks, G., 2020. Siberian and temperate ecosystems shape Northern Hemisphere atmospheric CO2 seasonal amplification. Proc. Natl. Acad. Sci. 117, 21079–21087. https://doi.org/10.1073/pnas.1914135117

Linder, P., Jonsson, P., Niklasson, M., 1998. Tree mortality after prescribed burning in an old-growth Scots pine forest in northern Sweden. Silva Fenn. 32. https://doi.org/10.14214/sf.675

Liu, Y.Y., Dijk, A.I.J.M. van, Jeu, R.A.M. de, Canadell, J.G., McCabe, M.F., Evans, J.P., Wang, G., 2015. Recent reversal in loss of global terrestrial biomass. Nat. Clim. Change 5, 470–474. https://doi.org/10.1038/nclimate2581

Lizundia-Loiola, J., Otón, G., Ramo, R., Chuvieco, E., 2020. A spatio-temporal active-fire clustering approach for global burned area mapping at 250 m from MODIS data. Remote Sens. Environ. 236, 111493. https://doi.org/10.1016/j.rse.2019.111493

Malevsky-Malevich, S.P., Molkentin, E.K., Nadyozhina, E.D., Shklyarevich, O.B., 2008. An assessment of potential change in wildfire activity in the Russian boreal forest zone induced by climate warming during the twenty-first century. Clim. Change 86, 463–474. https://doi.org/10.1007/s10584-007-9295-7

Mouillot, F., Schultz, M.G., Yue, C., Cadule, P., Tansey, K., Ciais, P., Chuvieco, E., 2014. Ten years of global burned area products from spaceborne remote sensing—A review: Analysis of user needs and recommendations for future developments. Int. J. Appl. Earth Obs. Geoinformation 26, 64–79. https://doi.org/10.1016/j.jag.2013.05.014

Myers-Smith, I.H., Forbes, B.C., Wilmking, M., Hallinger, M., Lantz, T., Blok, D., Tape, K.D., Macias-Fauria, M., Sass-Klaassen, U., Lévesque, E., Boudreau, S., Ropars, P., Hermanutz, L., Trant, A., Collier, L.S., Weijers, S., Rozema, J., Rayback, S.A., Schmidt, N.M., Schaepman-Strub, G., Wipf, S., Rixen, C., Ménard, C.B., Venn, S., Goetz, S., Andreu-Hayles, L., Elmendorf, S., Ravolainen, V., Welker, J., Grogan, P., Epstein, H.E., Hik, D.S., 2011. Shrub expansion in tundra ecosystems: dynamics, impacts and research priorities. Environ. Res. Lett. 6, 045509. https://doi.org/10.1088/1748-9326/6/4/045509

Natole, M., Ying, Y., Buyantuev, A., Stessin, M., Buyantuev, V., Lapenis, A., 2021. Patterns of mega-forest fires in east Siberia will become less predictable with climate warming. Environ. Adv. 4, 100041. https://doi.org/10.1016/j.envadv.2021.100041

Noce, S., Caporaso, L., Santini, M., 2019. Climate Change and Geographic Ranges: The Implications for Russian Forests. Front. Ecol. Evol. 7, 57. https://doi.org/10.3389/fevo.2019.00057

Pan, Y., Birdsey, R.A., Fang, J., Houghton, R., Kauppi, P.E., Kurz, W.A., Phillips, O.L., Shvidenko, A., Lewis, S.L., Canadell, J.G., Ciais, P., Jackson, R.B., Pacala, S.W., McGuire, A.D., Piao, S., Rautiainen, A., Sitch, S., Hayes, D., 2011. A Large and Persistent Carbon Sink in the World's Forests. Science 333, 988–993. https://doi.org/10.1126/science.1201609

Paramonov, E.G., Ishutin, Ya.N., 1999. Large Fires in Altai Krai (Barnaul, 1999) [in Russian].

Payette, S., Delwaide, A., 2003. Shift of Conifer Boreal Forest to Lichen–Heath Parkland Caused by Successive Stand Disturbances. Ecosystems 6, 540–550. https://doi.org/10.1007/PL00021507

Pedregosa, F., Varoquaux, G., Gramfort, A., Michel, V., Thirion, B., Grisel, O., Blondel, M., Prettenhofer, P., Weiss, R., Dubourg, V., Vanderplas, J., Passos, A., Cournapeau, D., Brucher, M., Perrot, M., Duchesnay, É., 2011. Scikit-learn: Machine Learning in Python. J. Mach. Learn. Res. 12, 2825–2830.

Perrault-Hébert, M., Boucher, Y., Fournier, R., Girard, F., Auger, I., Thiffault, N., Grenon, F., 2017. Ecological drivers of post-fire regeneration in a recently managed boreal forest landscape of eastern Canada. For. Ecol. Manag. 399, 74–81. https://doi.org/10.1016/j.foreco.2017.05.026

Ponomarev, E., Yakimov, N., Ponomareva, T., Yakubailik, O., Conard, S.G., 2021. Current Trend of Carbon Emissions from Wildfires in Siberia. Atmosphere 12, 559. https://doi.org/10.3390/atmos12050559

Ponomarev, E.I., Kharuk, V.I., Ranson, K.J., 2016. Wildfires Dynamics in Siberian Larch Forests. Forests 7, 125. https://doi.org/10.3390/f7060125

Potapov, P., Hansen, M.C., Laestadius, L., Turubanova, S., Yaroshenko, A., Thies, C., Smith, W., Zhuravleva, I., Komarova, A., Minnemeyer, S., Esipova, E., 2017. The last frontiers of wilderness: Tracking loss of intact forest landscapes from 2000 to 2013. Sci. Adv. 3, e1600821. https://doi.org/10.1126/sciadv.1600821

Potapov, P., Hansen, M.C., Stehman, S.V., Loveland, T.R., Pittman, K., 2008. Combining MODIS and Landsat imagery to estimate and map boreal forest cover loss. Remote Sens. Environ. 112, 3708–3719. https://doi.org/10.1016/j.rse.2008.05.006

Qin, Y., Abatzoglou, J.T., Siebert, S., Huning, L.S., AghaKouchak, A., Mankin, J.S., Hong, C., Tong, D., Davis, S.J., Mueller, N.D., 2020. Agricultural risks from changing snowmelt. Nat. Clim. Change 10, 459–465. https://doi.org/10.1038/s41558-020-0746-8

Randerson, J.T., Chen, Y., Werf, G.R. van der, Rogers, B.M., Morton, D.C., 2012. Global burned area and biomass burning emissions from small fires. J. Geophys. Res. Biogeosciences 117. https://doi.org/10.1029/2012JG002128

Randerson, J.T., van der Werf, G.R., Giglio, L., Collatz, G.J., Kasibhatla, P.S., 2017. Global Fire Emissions Database, Version 4.1 (GFEDv4) 1925.7122549999906 MB. https://doi.org/10.3334/ORNLDAAC/1293

Rogers, B.M., Balch, J.K., Goetz, S.J., Lehmann, C.E.R., Turetsky, M., 2020. Focus on changing fire regimes: interactions with climate, ecosystems, and society. Environ. Res. Lett. 15, 030201. https://doi.org/10.1088/1748-9326/ab6d3a

Rogers, B.M., Soja, A.J., Goulden, M.L., Randerson, J.T., 2015. Influence of tree species on continental differences in boreal fires and climate feedbacks. Nat. Geosci. 8, 228–234. https://doi.org/10.1038/ngeo2352

Sanderson, B.M., Fisher, R.A., 2020. A fiery wake-up call for climate science. Nat. Clim. Change 10, 175–177. https://doi.org/10.1038/s41558-020-0707-2

Sandström, J., Edman, M., Jonsson, B.G., 2020. Rocky pine forests in the High Coast Region in Sweden: structure, dynamics and history. Nat. Conserv. 38, 101.

Sannikov, S.N., Sannikova, N.S., Petrova, I.V., Cherepanova, O.E., 2020. The forecast of fire impact on Pinus sylvestris renewal in southwestern Siberia. J. For. Res. https://doi.org/10.1007/s11676-020-01260-1

Schulze, E.-D., Wirth, C., Mollicone, D., von Lüpke, N., Ziegler, W., Achard, F., Mund, M., Prokushkin, A., Scherbina, S., 2012. Factors promoting larch dominance in central Siberia: fire versus growth performance and implications for carbon dynamics at the boundary of evergreen and deciduous conifers. Biogeosciences 9, 1405–1421. https://doi.org/10.5194/bg-9-1405-2012

Schulzweida, U., 2020. CDO User Guide. https://doi.org/10.5281/zenodo.5614769

Shuman, J.K., Foster, A.C., Shugart, H.H., Hoffman-Hall, A., Krylov, A., Loboda, T., Ershov, D., Sochilova, E., 2017. Fire disturbance and climate change: implications for Russian forests. Environ. Res. Lett. 12, 035003. https://doi.org/10.1088/1748-9326/aa5eed

Shvetsov, E.G., Kukavskaya, E.A., Buryak, L.V., 2016. Satellite monitoring of the state of forest vegetation after fire impacts in the Zabaikal region. Contemp. Probl. Ecol. 9, 702–710. https://doi.org/10.1134/S1995425516060123

Shvetsov, E.G., Kukavskaya, E.A., Buryak, L.V., Barrett, K., 2019. Assessment of post-fire vegetation recovery in Southern Siberia using remote sensing observations. Environ. Res. Lett. 14, 055001. https://doi.org/10.1088/1748-9326/ab083d

Shvetsov, E.G., Kukavskaya, E.A., Shestakova, T.A., Laflamme, J., Rogers, B.M., 2021. Increasing fire and logging disturbances in Siberian boreal forests: a case study of the Angara region. Environ. Res. Lett. 16, 115007. https://doi.org/10.1088/1748-9326/ac2e37

Sidoroff, K., Kuuluvainen, T., Tanskanen, H., Vanha-Majamaa, I., 2007. Tree mortality after low-intensity prescribed fires in managed Pinus sylvestris stands in southern Finland. Scand. J. For. Res. 22, 2–12. https://doi.org/10.1080/02827580500365935

Sizov, O., Ezhova, E., Tsymbarovich, P., Soromotin, A., Prihod’ko, N., Petäjä, T., Zilitinkevich, S., Kulmala, M., Bäck, J., Köster, K., 2021. Fire and vegetation dynamics in northwest Siberia during the last 60 years based on high-resolution remote sensing. Biogeosciences 18, 207–228. https://doi.org/10.5194/bg-18-207-2021

Smets, B., Tansey, K., Wolfs, D., Jacobs, T., 2017. PRODUCT USER MANUAL BURNED AREA AND SEASONALITY COLLECTION 300M VERSION 1.

Soja, A., Shugart, H., Sukhinin, A., Conard, S., Stackhouse Jr, P., 2006. Satellite-Derived Mean Fire Return Intervals As Indicators Of Change In Siberia (1995–2002). Mitig. Adapt. Strateg. Glob. Change 11, 75–96. https://doi.org/10.1007/s11027-006-1009-3

Srivastava, A., Grotjahn, R., Ullrich, P.A., 2020. Evaluation of historical CMIP6 model simulations of extreme precipitation over contiguous US regions. Weather Clim. Extrem. 29, 100268. https://doi.org/10.1016/j.wace.2020.100268

Stavrova, N.I., Gorshkov, V.V., Katjutin, P.N., Bakkal, I.J., 2020. The Structure of Northern Siberian Spruce–Scots Pine Forests at Different Stages of Post-Fire Succession. Forests 11, 558. https://doi.org/10.3390/f11050558

Stevens-Rumann, C.S., Kemp, K.B., Higuera, P.E., Harvey, B.J., Rother, M.T., Donato, D.C., Morgan, P., Veblen, T.T., 2018. Evidence for declining forest resilience to wildfires under climate change. Ecol. Lett. 21, 243–252. https://doi.org/10.1111/ele.12889

Stralberg, D., Wang, X., Parisien, M.-A., Robinne, F.-N., Sólymos, P., Mahon, C.L., Nielsen, S.E., Bayne, E.M., 2018. Wildfire-mediated vegetation change in boreal forests of Alberta, Canada. Ecosphere 9, e02156. https://doi.org/10.1002/ecs2.2156

Suarez, F., Binkley, D., Kaye, M.W., Stottlemyer, R., 1999. Expansion of forest stands into tundra in the Noatak National Preserve, northwest Alaska. Écoscience 6, 465–470. https://doi.org/10.1080/11956860.1999.11682538

Sullivan, Janet., 1993. Pinus sylvestris. [WWW Document]. Fire Eff. Inf. Syst. Online US Dep. Agric. For. Serv. Rocky Mt. Res. Stn. Fire Sci. Lab. Prod. URL https://www.fs.fed.us/database/feis/plants/tree/pinsyl/all.html (accessed 3.5.21).

Tepley, A.J., Thomann, E., Veblen, T.T., Perry, G.L.W., Holz, A., Paritsis, J., Kitzberger, T., Anderson-Teixeira, K.J., 2018. Influences of fire–vegetation feedbacks and post-fire recovery rates on forest landscape vulnerability to altered fire regimes. J. Ecol. 106, 1925–1940. https://doi.org/10.1111/1365-2745.12950

Theil, H., 1950. A rank-invariant method of linear and polynomial regression analysis, Part 3. Presented at the Proceedings of Koninalijke Nederlandse Akademie van Weinenschatpen A, pp. 1397–1412.

Tomshin, O., Solovyev, V., 2021. Spatio-temporal patterns of wildfires in Siberia during 2001–2020. Geocarto Int. 0, 1–19. https://doi.org/10.1080/10106049.2021.1973581

van der Werf, G.R., Randerson, J.T., Giglio, L., van Leeuwen, T.T., Chen, Y., Rogers, B.M., Mu, M., van Marle, M.J.E., Morton, D.C., Collatz, G.J., Yokelson, R.J., Kasibhatla, P.S., 2017. Global fire emissions estimates during 1997–2016. Earth Syst. Sci. Data 9, 697–720. https://doi.org/10.5194/essd-9-697-2017

Walker, X.J., Rogers, B.M., Veraverbeke, S., Johnstone, J.F., Baltzer, J.L., Barrett, K., Bourgeau-Chavez, L., Day, N.J., de Groot, W.J., Dieleman, C.M., Goetz, S., Hoy, E., Jenkins, L.K., Kane, E.S., Parisien, M.-A., Potter, S., Schuur, E. a. G., Turetsky, M., Whitman, E., Mack, M.C., 2020. Fuel availability not fire weather controls boreal wildfire severity and carbon emissions. Nat. Clim. Change 10, 1130–1136. https://doi.org/10.1038/s41558-020-00920-8

Wan, X., 2019. Influence of feature scaling on convergence of gradient iterative algorithm. J. Phys. Conf. Ser. 1213, 032021. https://doi.org/10.1088/1742-6596/1213/3/032021

Whitman, E., Parisien, M.-A., Thompson, D.K., Flannigan, M.D., 2019. Short-interval wildfire and drought overwhelm boreal forest resilience. Sci. Rep. 9, 1–12. https://doi.org/10.1038/s41598-019-55036-7

Wilks, D.S., 2016. “The Stippling Shows Statistically Significant Grid Points”: How Research Results are Routinely Overstated and Overinterpreted, and What to Do about It. Bull. Am. Meteorol. Soc. 97, 2263–2273. https://doi.org/10.1175/BAMS-D-15-00267.1

Wright, J.W., Wilson, L.F., Randall, W.K., 1967. Differences Among Scotch Pine Varieties in Susceptibility to European Pine Sawfly. For. Sci. 13, 175–181. https://doi.org/10.1093/forestscience/13.2.175

Yue, S., Pilon, P., Cavadias, G., 2002. Power of the Mann–Kendall and Spearman's rho tests for detecting monotonic trends in hydrological series. J. Hydrol. 259, 254–271. https://doi.org/10.1016/S0022-1694(01)00594-7

Zheng, A., Casari, A., 2018. Feature Engineering for Machine Learning: Principles and Techniques for Data Scientists. O'Reilly Media, Inc.